


2019

Measurement precision and reliability of supraspinatus tendon strain using speckle track analysis of ultrasound images

Gregory Alan McClanahan
gamccclan@gmail.com

Follow this and additional works at: <https://mds.marshall.edu/etd>

 Part of the [Analytical, Diagnostic and Therapeutic Techniques and Equipment Commons](#), and the [Musculoskeletal, Neural, and Ocular Physiology Commons](#)

Recommended Citation

McClanahan, Gregory Alan, "Measurement precision and reliability of supraspinatus tendon strain using speckle track analysis of ultrasound images" (2019). *Theses, Dissertations and Capstones*. 1206.
<https://mds.marshall.edu/etd/1206>

This Thesis is brought to you for free and open access by Marshall Digital Scholar. It has been accepted for inclusion in Theses, Dissertations and Capstones by an authorized administrator of Marshall Digital Scholar. For more information, please contact zhangj@marshall.edu, beachgr@marshall.edu.

**MEASUREMENT PRECISION AND RELIABILITY OF SUPRASPINATUS TENDON
STRAIN USING SPECKLE TRACK ANALYSIS OF ULTRASOUND IMAGES.**

A thesis submitted to
the Graduate College of
Marshall University
In partial fulfillment of
the requirements for the degree of
Master of Science

In

Biomechanics

by

Gregory Alan McClanahan

Approved by

Dr. Mark K. Timmons, Committee Chairperson

Dr. Suzanne Konz

Dr. Steven Leigh

Marshall University

August 2019

APPROVAL OF THESIS

We, the faculty supervising the work of Gregory Alan McClanahan, affirm that the thesis, *Measurement Precision and Reliability of Supraspinatus Tendon Strain Using Speckle Track Analysis of Ultrasound Images*, meets the high academic standards for original scholarship and creative work established by the Master of Science in Biomechanics and the College of Health Professions. This work also conforms to the editorial standards of our discipline and the Graduate College of Marshall University. With our signatures, we approve the manuscript for publication.



7-18-2019

Dr. Mark K. Timmons, PhD, ATC, School of Kinesiology, Committee Chairperson

Date



July 18, 2019

Dr. Suzanne Konz, PhD, ATC, CSCS, School of Kinesiology, Committee Member

Date



July 18th, 2019

Dr. Steven Leigh, PhD, AMInstP, School of Kinesiology, Committee Member

Date

© 2019
Gregory Alan McClanahan
ALL RIGHTS RESERVED

ACKNOWLEDGMENTS

I wish to express my gratitude to the faculty of the Marshall University School of Kinesiology. I would like to thank my committee members: Dr. Mark Timmons, Dr. Suzanne Konz, and Dr. Steven Leigh for providing excellent support and feedback throughout the course of this project and my time at Marshall University. I would also like to thank the following people for their support in helping me collect data: Elle Sheen, Mackenzie Holderby, Jared Bradley, and Heather Tolnay. Finally, I would like to express my appreciation of my incredible family and friends for supporting me in my pursuit of higher education.

TABLE OF CONTENTS

List of Tables	viii
List of Figures	ix
Abstract	xi
Chapter 1	1
Introduction	1
Purpose	4
Research Question	4
Hypotheses	4
Limitations	4
Delimitations	4
Assumptions	5
Operational Definitions	5
Chapter 2	6
Literature review	6
Background	6
Tendon	8
Ultrasound	10
Speckle Tracking	12
Strain	14
Conclusion	16
Chapter 3	17
Methods	17

Participants.....	17
Participant Information	17
IRB Consideration	17
Inclusion Criteria	18
Exclusion Criteria	18
Pilot Study.....	18
Instrumentation	18
Protocol.....	19
Procedures.....	21
Demographics	21
Self-Reported Outcome Measures	22
Physical Examination.....	22
Manual Muscle Strength.....	22
External rotation.....	23
Internal rotation.....	23
Shoulder abduction	23
Shoulder Clinical Tests	24
Glenohumeral Stability	24
Apprehension Relocation.....	24
Anterior Release.....	24
Sulcus Sign.....	25
Rotator Cuff Pathology	25
Painful Arc Test	25

Neer Test.....	25
Kennedy Hawkins Test.....	25
Ultrasound Imaging	26
Phase 1 Standard Ultrasound Assessment	26
Phase 2 Ultrasound for Speckle Tracking.....	27
Speckle Tracking	30
Statistical Analysis.....	41
Chapter 4.....	43
Results.....	43
Intra Images	43
Inter Images	44
Bland-Altman Plots.....	46
Chapter 5.....	61
Discussion.....	61
Limitations	68
Future Research	70
Conclusion	70
References.....	72
Appendix A: IRB Approval.....	79
Appendix B: Consent Form	80

LIST OF TABLES

Table 1. Participant Demographic Data.....	17
Table 2. Intra Image Results, Longitudinal-Strain.....	44
Table 3. Intra Image Results, Axial-Strain	44
Table 4. Inter Image Results, Longitudinal-Strain.....	45
Table 5. Inter Image Results, Axial-Strain	46
Table 6. T-tests of strain values between image 1 and image 2	47
Table 7. T-tests of strain values between image 1 and image 5	48

LIST OF FIGURES

Figure 1. Longitudinal Ultrasound Image of Supraspinatus tendon	20
Figure 2. Strain Direction and Tendon Position Labels.....	21
Figure 3. Data collection with Ultrasound Transducer (Photo by Dr. Mark Timmons).....	28
Figure 4. Force Transducer Placement, Wrist View (Photo by Dr. Mark Timmons).....	28
Figure 5. Scapula Stabilization, Side View (Photo by Dr. Mark Timmons)	29
Figure 6. Data Collection Setup (Photo by Dr. Mark Timmons).....	30
Figure 7. Reference and Current Images Set	31
Figure 8. Region of Interest	31
Figure 9. After Region of Interest is Set	32
Figure 10. DIC Parameters	33
Figure 11. After DIC Parameters are Set	34
Figure 12. Setting Seed	35
Figure 13. Seed Preview, After Setting Seed.....	35
Figure 14. After DIC Analysis is Complete.....	36
Figure 15. Formatting Displacements.....	37
Figure 16. After Displacements are Formatted.....	37
Figure 17. Setting Strain Parameters	38
Figure 18. After Strains are Calculated.....	39
Figure 19. Longitudinal (x) Direction Strain Map.....	40
Figure 20. Axial Direction Strain Map	41
Figure 21. Bland-Altman of Bursal side Axial strains for Image 1 and Image 2	49
Figure 22. Bland-Altman of Mid-substance Axial strains for Image 1 and Image 2.....	50

Figure 23. Bland-Altman of Joint side Axial strains for Image 1 and Image 2.....	51
Figure 24. Bland-Altman of Bursal side Longitudinal strains for Image 1 and Image 2	52
Figure 25. Bland-Altman of Mid-substance Longitudinal strains for Image 1 and Image 2.....	53
Figure 26. Bland-Altman of Joint side Longitudinal strains for Image 1 and Image 2	54
Figure 27. Bland-Altman of Bursal side Axial strains for Image 1 and Image 5	55
Figure 28. Bland-Altman of Mid-substance Axial strains for Image 1 and Image 5.....	56
Figure 29. Bland-Altman of Joint side Axial strains for Image 1 and Image 5	57
Figure 30. Bland-Altman of Bursal side Longitudinal strains for Image 1 and Image 5	58
Figure 31. Bland-Altman of Mid-substance Longitudinal strains for Image 1 and Image 5.....	59
Figure 32. Bland-Altman of Joint side Longitudinal strains for Image 1 and Image 5	60

ABSTRACT

Introduction: Ultrasound speckle tracking is an emergent method in studying musculoskeletal physiology and disease. For a method to be effective and useful, it needs to be precise and reliable. The precision and reliability of supraspinatus tendon strain measurements have not been explored. The purpose of this study was to examine the precision and reliability of speckle tracking to measure supraspinatus tendon strain.

Methods: Forty-two (42) participants participated in this study. Five (5) ultrasound images of the participant's right shoulder supraspinatus tendon were collected during a maximal voluntary isometric abduction contraction. Cine loop video files of the 5 imaging trials were imported into Ncorr software for speckle track analysis. Axial and longitudinal strain measurements were made for the bursal side (top), mid-substance (middle), and joint side (bottom) of the thickest portion of the supraspinatus tendon. Reliability of the strain measures was determined using interclass correlation coefficients (ICC), the precision of the strain measures was determined using the standard error of measure (SEM) and minimal detectable change (MDC). Bland-Altman plots were created in order to explore systematic error.

Results: Mean strain of the supraspinatus tendon ranged from 1.791 to -2.120 %. The ICC values for the longitudinal and axial strains of both within and between images was high (>0.9) for all locations of the tendon (bursal side, mid-substance, and joint side), which demonstrates very good reliability. The 95% confidence interval for the MDC was large for all measurements of strain, except the axial strain at the mid-substance, which demonstrates poor precision. Review of the Bland-Altman plots revealed some systematic error for the longitudinal strain of the bursal side of the supraspinatus tendon.

Conclusions: The results of the investigation show evidence of very good reliability, poor precision, and some evidence of systematic error. The very good ICC values support the hypothesis that speckle tracking does produce reliable strain measurements. The large MDC values do not support the hypothesis that speckle tracking produces precise strain measurements. Improvements in ultrasound image quality and the shoulder stabilization process need to be made before ultrasound speckle tracking will be a viable research method for the supraspinatus tendon.

CHAPTER 1

INTRODUCTION

The complexity of the shoulder anatomy poses challenges in the assessment and treatment of shoulder injury. Ultrasound imaging is used to make measurements of the shoulder anatomy in vivo in order to assist in the assessment of shoulder injury (Cholewinski, Kusz, Wojciechowski, Cielinski, & Zoladz, 2008; Crass, Craig, Bretzke, & Feinberg, 1985; Martinoli, 2010). Diagnostic ultrasound uses the reflection of sound waves from anatomical structures, to form an image of the anatomy (Venables, 2011). Quantitative and qualitative assessments of the anatomy are made using ultrasound imaging (Cholewinski et al., 2008; Crass et al., 1985). Qualitative assessments are based on subjective observation of image appearance while quantitative measures are based on objective empirical data. Improvements in the ultrasound imaging techniques should improve the assessment of shoulder injuries.

Tendinopathy of the rotator cuff complex is the leading cause of shoulder pain in many clinical populations, and tendinopathy of the rotator cuff complex is greatly affected by its anatomy (Luime et al., 2004; Van Der Windt, Koes, De Jong, & Bouter, 1995; Vecchio, Kavanagh, Hazleman, & King, 1995). The supraspinatus tendon connects to the supraspinatus muscle to the greater tubercle of the humerus. The activity of the supraspinatus aids in arm abduction. The supraspinatus tendon traverses through the subacromial space, under the acromion and above the humeral head. Contraction of the supraspinatus results in an increase in the stress within the tendon while decreases in the width of the subacromial spaces leads to increased compression of the supraspinatus tendon within the subacromial space (Clark & Harryman, 1992; Dugas, Campbell, Warren, Robie, & Millett, 2002; Roh et al., 2000). Tendon is a viscoelastic material, so tendon does not necessarily have a linear deformation response to

stress. The stress within the tendon causes special deformation, leading to strain, which is the percent change in original length of a structure. The supraspinatus tendon curves and twists over the head of the humerus before inserting into the greater tubercle of the humerus (Clark & Harryman, 1992; Dugas et al., 2002; Roh et al., 2000). The stress leads to the development of tendinopathy (Andarawis-Puri, Ricchetti, & Soslowsky, 2009; Magnusson, Langberg, & Kjaer, 2010; Miller, Fujimaki, Araki, Musahl, & Debski, 2014). The anatomy of the supraspinatus tendon produces difficulty making ultrasound images of the tendon since the tendon cannot be imaged as a straight segment and no single image can form the entire tendon. Ultrasound is used to make measurements since it is non-invasive and quick to perform (Venables, 2011). Improvement in the ultrasound imaging techniques could improve the assessment of injury to the supraspinatus tendon by allowing researchers and clinicians an effective way to measure strain.

To perform more thorough assessments of the shoulder, quantitative values beyond dimensions of tissue need to be obtained. Diagnostic ultrasound can be used with a method called speckle tracking to make new quantitative in vivo measurements of muscle and tendon. The values that are obtained from speckle tracking can then be used to determine important clinical factors that can be used to assess the shoulder, such as risk for muscle or tendon strain. Having actual numbers from the speckle tracking method that allow for a quantitative assessment will allow researchers and clinicians to make conclusions that are based on objective measurement rather than subjective information. The values from measurements that are determined from a method need to be precise and reliable, which means that a measurement should have low error and high consistency. Speckle tracking, to be a useful and effective method, must be precise and reliable.

Speckle tracking is a method that uses changes in the position of greyscale color pixels of ultrasound images to measure changes in tissue position over time (Korstanje, Selles, Stam, Hovius, & Bosch, 2010; Revell, Mirmehdi, & McNally, 2005). Speckle tracking has for several years been used in echocardiography to make in vivo measurements and assessments of the heart for both researchers and clinicians (Amundsen et al., 2006; Marwick et al., 2009). More recently, speckle tracking has been used to make measurements on tendon and non-cardiac muscle tissue. Speckle tracking is an ultrasound-based quantitative method that might aid in the assessment of shoulder injury. Speckle tracking has many uses in the lab and clinically; such as measuring the strain of muscle or tendon, which is the percent change in length of a material. The focus of previous muscle and tendon studies has been on the strain and strain rate of muscle and tendon of the wrist, knee, and lower leg; which is due to the ease at which a researcher or clinician can use ultrasound to capture an image or a video of muscle and tendon of the wrist, knee, and lower leg since each are superficial and straight (Pearson, Ritchings, & Mohamed, 2014; Slane, Bogaerts, Thelen, & Scheys, 2018; Slane & Thelen, 2015; Van Doesburg et al., 2012). Speckle tracking with ultrasound could be used to assess the strain of supraspinatus tendon, which may help researchers and clinicians in the study of mechanisms and treatment of shoulder injury.

Ultrasound is a commonly used instrument to make in vivo measurements of the shoulder for assessment of injuries and pain (Cholewinski et al., 2008; Crass et al., 1985). Speckle tracking, in the measurement of tendon strain, is an emergent method that is used with ultrasound to make new in vivo measurements of tendon and muscle, such as the Achilles tendon (Pearson et al., 2014; Slane et al., 2018; Slane & Thelen, 2015; Van Doesburg et al., 2012). Methods must be precise, or have low error, and reliable, or have high consistency, to give researchers and

clinicians confidence in measurements. However, the precision and reliability of supraspinatus tendon strain measurements has not been explored. Determining the precision and reliability of supraspinatus strain measures using speckle tracking analysis of ultrasound images will help researchers and clinicians to make new and better assessments of the shoulder.

Purpose

The purpose of this study was to examine the reliability and precision of speckle tracking to measure supraspinatus tendon strain.

Research Question

Does speckle tracking produce a reliable and precise measurement of tendon strain during static loading of the supraspinatus tendon?

Hypotheses

Null Hypothesis (H_0): Speckle tracking does not produce a reliable or precise measurement of strain for static loads of the supraspinatus tendon.

Alternative Hypothesis (H_{A1}): Speckle tracking does produce a reliable measurement of strain for static loads of the supraspinatus tendon.

Alternative Hypothesis (H_{A2}): Speckle tracking does produce a precise measurement of strain for static loads of the supraspinatus tendon.

Limitations

1. Unknown asymptomatic shoulder pathology
2. Physical activity prior to testing will not be controlled
3. Size and depth of participant's tendons will not be controlled

Delimitations

1. Participants did not have any shoulder pain or injury

2. Participants were between the ages of 18 and 29
3. Participants were not obese or overweight

Assumptions

1. Tendon strain is normally distributed for the samples drawn
2. Participants are independent
3. Tendon strain variance of the population is homogenous
4. The sample is representative of their corresponding population
5. Participants will provide honest responses about history of upper limb pain and injury

Operational Definitions

1. MATLAB – Programming Language and software, used for data analysis.
2. Ncorr – An open source software package used with MATLAB to perform speckle tracking analysis.
3. Speckle Tracking – A method of tracking movement of a series of images by following patterns in greyscale images (Korstanje et al., 2010; Revell et al., 2005).
4. Stress – An internal measure of force per unit area, a pressure, of a material or mass (Tada, Paris, & Irwin, 2000).
5. Strain – Relative change in the distance between two portions or areas of a material or mass (Andarawis-Puri et al., 2009).
6. Precision – The degree to which a measurement varies.
7. Reliability – The consistency of making a measurement.

CHAPTER 2

LITERATURE REVIEW

The validity of supraspinatus tendon strain measurements has not been explored with ultrasound speckle tracking. The purpose of this study was to examine the precision and reliability of strain measurements made using speckle track analysis of ultrasound images speckle tracking. It is hypothesized that speckle tracking does produce a reliable or precise measurement of strain for static loads of the supraspinatus tendon.

Background

Tendon, which is an elastic-like tissue that connects muscle to bone, not only serves to store and release energy during the stretch-shorten cycle, but also absorbs transmitted force to prevent injury (Alexander, 2002; Taylor, Dalton, Seaber, & Garrett, 1990; Willems, Cavagna, & Heglund, 1995; Zajac, 1989). The supraspinatus tendon, which is a part of the rotator cuff, is particularly important for glenohumeral abduction and stabilization. Many mechanisms lead to the development of supraspinatus injury (Seitz, McClure, Finucane, Boardman, & Michener, 2011; Seitz & Michener, 2011). The supraspinatus tendon may be a contributor to the development of shoulder impingement syndrome (Cholewinski et al., 2008; Crass et al., 1985; McCreesh, Purtill, Donnelly, & Lewis, 2017; Michener, Subasi Yesilyaprak, Seitz, Timmons, & Walsworth, 2013). Investigating how to evaluate healthy and pathologic supraspinatus tendon is necessary, if the causes and effects of rotator cuff disease and injuries are to be understood.

Diagnostic ultrasound is a method that uses an ultrasonic transducer, which transmits ultrasonic waves into the body and receives ultrasonic waves from the body, to make in vivo measurements through imaging the human body (Venables, 2011). Clinicians and researchers have used diagnostic ultrasound to evaluate healthy and pathological tendon. Researchers and

clinicians do this by making quantitative and qualitative assessments of the anatomy they are investigating (Cholewinski et al., 2008; Crass et al., 1985; Martinoli, 2010). Diagnostic ultrasound can be used to investigate healthy and pathologic supraspinatus tendon. These investigations have included studying how the supraspinatus tendon size is different for participant with shoulder impingement syndrome and participant who went through fatiguing protocol (Cholewinski et al., 2008; Crass et al., 1985). Diagnostic ultrasound has been used to study strain in tendon and muscle; however, there is little to no study of strain with diagnostic ultrasound of the supraspinatus tendon.

Speckle tracking, an ultrasound-based technique, has been used by researchers and clinicians to study the human body. Researchers have found evidence that suggests speckle tracking is a valid method for in vivo strain measurements of the human body (Korstanje et al., 2010; Revell et al., 2005). Speckle tracking has been primarily used to evaluate function and strain of cardiac tissue and muscle and tendon of the wrist, knee, and lower leg (Amundsen et al., 2006; Marwick et al., 2009; Pearson et al., 2014; Slane et al., 2018; Slane & Thelen, 2015; Van Doesburg et al., 2012). Speckle tracking could be used to investigate the health and function of shoulder tendon.

Strain, a critical factor for tendon evaluation, can be measured in multiple axes with speckle tracking. Tendon tears have been observed to correlate with increased minimum and maximum principal strain, which is strain linear to a given axis (Andarawis-Puri et al., 2009; Miller et al., 2014). Furthermore, this increased strain leads to larger tearing which occurs along the axis of the strain (Andarawis-Puri et al., 2009; Miller et al., 2014). In rat tendon that cyclic loading, principal axis strains, leads to increased collagen production, while over-loading or

long-term loading can cause damage (Maeda, Shelton, Bader, & Lee, 2007; Richardson, Kegerreis, Thomopoulos, & Holmes, 2018; Screen, Shelton, Bader, & Lee, 2005).

Evaluating rotator cuff tear etiology is complex; but, examining the precision and reliability of an emergent method, speckle tracking, is important for making new, valuable measurements to assess the supraspinatus tendon for injury prevention and rehabilitative care. This review will comprise a comprehensive account of the available literature on supraspinatus tendon epidemiology, ultrasound theory in application to evaluating tendons, speckle tracking theory and its relevance to studying tendon, and the relationship between stress and tendon morphology.

Tendon

Healthy tendon acts as an elastic medium, like a spring, to transfer forces from muscle to bone while storing energy to be released later. This energy storage and release cycle is completed by means of a stretch-shorten cycle (Alexander, 2002; Taylor et al., 1990; Willems et al., 1995; Zajac, 1989). Evidence suggests that during the stretch-shortening cycle frictional resistance is minimized in healthy tendon through the generation of a boundary lubrication regime (Theobald, Dowson, Khan, & Jones, 2012). The dry mass of tendon, the amount that is not liquid, makes up approximately 30% of the total mass. The dry mass is accounted for by collagen at approximately 86%, elastin at approximately 2%, and other components. Several types of collagen, each of which have different specific properties, are included in the total collagen composition of the dry mass of tendon (Jozsa & Kannus, 1997; Kjær et al., 2009). The supraspinatus tendon is made up of approximately 95% Type I collagen with the remainder primarily being Type III collagen with some small amounts of Types IV, V, VI, XII, and XIV (Bank, TeKoppele, Oostingh, Hazleman, & Riley, 1999; G. P. Riley et al., 1994).

The supraspinatus tendon is one of four main tendons that make up the rotator cuff, which wraps around the glenohumeral joint. The supraspinatus tendon connects the supraspinatus muscle, which originates from the supraspinatus fossa of the scapula, to its insertion at the greater tubercle of the humerus. As the supraspinatus muscle contracts and shortens, the supraspinatus tendon moves under the acromion (Clark & Harryman, 1992; Dugas et al., 2002; Roh et al., 2000). In healthy participants, between the ages of 18 and 40, the supraspinatus tendon had a mean maximum width of 14.9 mm in men and 13.5 mm in women, and the thickness of the tendon was 5.6 mm for men and 4.9 mm for women. Furthermore, no correlation between supraspinatus tendon measurements and participant height, weight, biceps thickness, or deltoid thickness was determined (Karthikeyan et al., 2014).

Tendon injuries can develop from repetitive movements or movements that cause excessive strain on the fibers of the tendon. Repetitive movements can lead to fatigue such that tendon tissue can become compromised and fail. Fatigue from repetitive movements results in the degradation of collagen proteins, which makes tendon more prone to tearing and therefore, increased strains. The specific mechanism for why injuries develop is not necessarily understood (Andarawis-Puri et al., 2009; Magnusson et al., 2010; Miller et al., 2014).

Two major pathologies of the shoulder, which are relevant to the supraspinatus tendon, are shoulder impingement syndrome and rotator cuff tear (Cholewicki et al., 2008; Crass et al., 1985; McCreesh et al., 2017; Michener et al., 2013). Shoulder impingement syndrome is the entrapment and compression of rotator cuff tendon under the acromion (Cholewicki et al., 2008; Crass et al., 1985; McCreesh et al., 2017; Michener et al., 2013). For healthy pain-free participants who underwent a fatiguing protocol, it was found that the mean supraspinatus tendon thickness increased compared to before the fatiguing protocol (Cholewicki et al., 2008; Crass et

al., 1985; McCreesh et al., 2017; Michener et al., 2013). Participants with subacromial impingement syndrome were found to have a thicker supraspinatus tendon and a larger distance between the infero-lateral edge of the acromion and the apex of the greater tuberosity of humerus (AGT distance) than asymptomatic control participant (Cholewinski et al., 2008; Crass et al., 1985; McCreesh et al., 2017; Michener et al., 2013). Rotator cuff tear, which can include a supraspinatus tendon tear, is the simple tearing or separating of connected fibers in the rotator cuff tendon. Rotator cuff tear can lead to further rotator cuff disease, such as rotator cuff tear arthropathy (Ecklund, Lee, Tibone, & Gupta, 2007).

The anatomy and structure of the supraspinatus tendon are critical for this study. During humeral elevation, the supraspinatus tendon will move under the acromion, which makes measurements difficult or even impossible. The supraspinatus tendon movement is a limitation of what can be studied. This limitation will not impact this study since the investigation is focused on if speckle tracking can be used on the supraspinatus tendon during an isometric contraction. The supraspinatus tendon will be investigated over a limited range of humeral elevation angles.

Ultrasound

Ultrasound is an imaging method that uses a transducer(s) to emit ultrasonic sound waves into the body which are scattered and receive some of the reflected signals that are scattered back toward the transducer. The transducer is connected to a machine that transforms the signal into an electromagnetic wave with piezoelectric crystals, converts the electromagnetic energy into a value, and reads the new value as a waveform. The reflected ultrasonic signal's characteristics of frequency, wavelength, amplitude, and direction depends on the characteristics, shape, and location of the tissue that is being imaged. The image type that is displayed by the ultrasound

machine depends on the selection of the researcher or clinician. B-mode type images, which are the standard black and white image used to view the shape and depth of tissue in the body, transform the reflected signal into a grey-scale image where pixel brightness is determined from the intensity of the reflected signal. Attenuation, which is the loss or decrease in intensity of signal as the sound travels deeper into tissue, is a significant concern when using ultrasound; however, this can be mitigated by decreasing the frequency of the emitted signal to achieve a higher signal penetration with decreased resolution. Conversely, a higher frequency of the emitted signal results in a higher resolution image that suffers from decreased penetration depth. Assumptions made when using ultrasound include: the speed of sound is constant, the emitted signal travels in a straight line along the axis of the transducer, the transducer beam has negligible thickness, and attenuation in all tissue is constant (Venables, 2011).

Diagnostic ultrasound is a common method used by researchers and clinicians to make in vivo measurements of the musculoskeletal system. Qualitative and quantitative assessments of injury, such as tendon tear or tissue geometry, are some of the most common uses of ultrasound (Cholewinski et al., 2008; Crass et al., 1985). Diagnostic ultrasound of the musculoskeletal system allows researchers and clinicians to make multiple assessments faster than other imaging techniques, such as MRI (Grassi, Filippucci, & Busilacchi, 2004; Wakefield et al., 2005).

In vivo measurements of the shoulder are a common use of diagnostic ultrasound in research. These measurements have been made to study and evaluate healthy and pathologic rotator cuff tendon. Many of these studies using ultrasound to evaluate the shoulder have focused on evaluating rotator cuff tendon. The supraspinatus tendon is a main focus in these studies, as it has implications for rotator cuff disease including rotator cuff tear, shoulder

impingement syndrome, and rotator cuff tear arthropathy (Cholewinski et al., 2008; Crass et al., 1985; Ecklund et al., 2007; Martinoli, 2010).

Diagnostic ultrasound is reliable and valid for imaging structures of the shoulder. The supraspinatus tendon has been reliably evaluated by researchers and clinicians with ultrasound. In this proposed study, ultrasound will be used for imaging of the supraspinatus tendon.

Speckle Tracking

Speckle tracking is a method that uses ultrasound imaging to measure displacement, and therefore strain and strain rates, of some tissue. Speckle tracking is done by tracking, the process of evaluating the correlation of an image from one frame to the next over a series of images or video, speckle, grey-scale pixels of the ultrasound image, throughout a movement or time. Block matching, which uses a defined region of interest as the initial block, tracks a block of speckle values over a movement or time (D'hooge, 2008; Korstanje et al., 2010; Mondillo et al., 2011; Revell et al., 2005). Strain and strain rate measurements can be made using block matching in speckle tracking by comparing multiple blocks initial and time-series displacements. Initial and time-series displacements can be used to find an initial length and the stretched length of tissue for each frame of the ultrasound images or video (Heimdal, 2008; Mondillo et al., 2011).

In vivo measurements of strain have been made with speckle tracking of cardiac tissue for several years (Amundsen et al., 2006; Marwick et al., 2009). Speckle tracking has more recently been used to study strain of muscle and tendon of human wrist, knee, and lower leg. These parts of the body have been investigated first as they have some of the easiest muscle and tendon to image with ultrasound (Pearson et al., 2014; Slane et al., 2018; Slane & Thelen, 2015; Van Doesburg et al., 2012). Since ultrasound and speckle tracking require a relatively stable, motionless set of images for researchers or clinicians to make accurate assessments, viewing a

relatively superficial and straight segment of tissue, such as the Achilles tendon is easier than a deep or curved segment of tissue, such as the supraspinatus tendon.

One study has used speckle tracking to analyze the supraspinatus tendon in vivo. In this study, for isotonic and isometric movements, superficial, middle, and deep tissue of the supraspinatus tendon had different displacements and, therefore, principal strains (Kim, Kim, Bigliani, Kim, & Jung, 2011). There are several concerns with the study including confusing or lack of descriptions on how the speckle tracking method was used, what type of ultrasound imaging was used, how strain was calculated, how the researchers used a spot or speckle, and the researcher's movement of the probe (Slagmolen et al., 2012). Although speckle tracking has been used to evaluate the supraspinatus tendon, there are concerns with the current use of, as well as a lack of evidence supporting the viability and reliability of, measurements made with speckle tracking. To quell these concerns, speckle tracking for use to study the supraspinatus tendon needs to be evaluated for precision and reliability of measurements.

Ncorr, a speckle tracking system based in MATLAB, allows the user to track movement from a reference image to subsequent images (Blaber, Adair, & Antoniou, 2015). The system is first opened by calling it within MATLAB. A reference image is set, which is the first ultrasound image before movement occurs. Current images, at least one but as many as you want, are then set into the program, which are the subsequent images to the reference image. The region of interest, which is the area of the images that you want to identify for speckle tracking and strain analysis, is set. DIC (Digital Image Correlation) parameters, including subset radius and spacing, are then set. Digital Image Correlation is a process by which subsets, specific points in the image that are tracked, from the reference image are correlated to subsets from the current images. The subsets that have the highest correlation are matched together, and

the difference in position of the subsets is the displacement (Ab Ghani, Ali, DharMalingam, & Mahmud, 2016). The radius and spacing determine how big and how dense the subsets appear. The DIC analysis is then run, which determines the displacements inside the region of interest. The displacements are then formatted, which allows the user to set units and determine the correlation coefficient minimum. Strain analysis is then performed, which determines the strains inside the region of interest from the displacements. The user can then plot and observe data present in the displacement or strain plots (Blaber et al., 2015).

There are many techniques and methods used by researchers and clinicians to evaluate the supraspinatus tendon; however, speckle tracking is unique in that it can be used to make non-invasive in vivo measurements of strain. Although speckle tracking has been used in other parts of the body for many years, there is a lack of evidence for its applicability or use in the supraspinatus tendon.

Strain

Tendon exists to transfer forces from muscle to bone by acting as an elastic medium which stores and releases energy by stretching and shortening, respectively. This elastic property of tendon decreases the total work needed for animals, including humans, to do to perform some action (Alexander, 2002; Taylor et al., 1990; Willems et al., 1995; Zajac, 1989). Forces transmitted to tendon from muscle cause strain, which is the change in length of a material from its initial condition, in multiple axes in tendon. In healthy shoulders, the supraspinatus muscle contracts to cause shoulder abduction by transmitting a force through the supraspinatus tendon to the humerus (Reed, Cathers, Halaki, & Ginn, 2013; Wickham, Pizzari, Stansfeld, Burnside, & Watson, 2010). The supraspinatus muscle contracts equally between the full-can exercise, abduction with the thumb pointed away from the body, and the empty-can

exercise, abduction with the thumb pointed toward the body (Reinold et al., 2007). These strains can lead to tendinopathy as well as characteristic changes of the material properties of the tendon (Arya & Kulig, 2010; G. Riley, 2004).

In rotator cuff tendon, percent increase in size of tendon tear is significantly correlated to an increased average minimum and maximum principal strain, where principal strain is on the axes parallel and orthogonal in plane to the image of the tendon (Andarawis-Puri et al., 2009). These increases in average minimum and maximum principal strain are associated with tears propagating from the initial tear toward the region with increased strain, which follows the direction the strain is highest (Andarawis-Puri et al., 2009; Miller et al., 2014). Increased transverse and shear strain of the rotator cuff at the attachment was observed in rats with localized defects compared to healthy controls (Locke et al., 2017). This increased strain suggests that healthy, non-defective rotator cuff tendon, supraspinatus tendon, resists failure, tearing, better than pathological or defective tendon, since the observed strain was increased for increased initial tendon tear size and defective tendon.

From a simulation that modeled loading of the human supraspinatus tendon, increased strain is predicted to lead to increased collagen production, the amount of collagen in the matrix, and damage, a decrease in the alignment of collagen fibers (Richardson et al., 2018). Increased collagen production in tendon was found in rat tails after cyclic loading, which lead to greater retention of newly synthesized matrix; however, long-term application of cyclic strain represented a decay effect in that the effects of loading were less marked (Maeda et al., 2007; Screen et al., 2005).

Strain plays a significant role in the study of tendon as it relates to injury occurrence and physical properties. In this proposed study precision and reliability strain measurements of the supraspinatus tendon with ultrasound speckle tracking will be investigated.

Conclusion

Supraspinatus tendon pathologies, such as rotator cuff tear, are arduous to study and evaluate. Researchers and clinicians have used ultrasound to evaluate the supraspinatus tendon. Speckle tracking is an ultrasound emergent method that has been used to study tendon in the human body. Measurements of strain, which are important for evaluating tendon, can be made with speckle tracking. Many researchers have used ultrasound speckle tracking to make strain measurements in human tendon; however, there is a dearth of evidence for making precise and reliable shoulder tendon, such as the supraspinatus tendon, measurements in humans. In this study, the precision and reliability of measuring static and loading conditions of the supraspinatus tendon with ultrasound speckle tracking will be examined.

CHAPTER 3

METHODS

Participants

Participant Information

Forty-one (41) healthy individuals participated in this study. No participants were excluded from the study, 17 participants were male, and 24 participants were female. Thirty-seven (37) participants were right hand dominant, 2 participants were left hand dominant, and 2 participants were ambidextrous. Participant demographic data can be found in Table 1.

Age (years)	22.2 ± 2.3
Weight (kg)	76.9 ± 18.6
Height (cm)	170.0 ± 9.5
PENN pain score	29.5 ± 1.2
PENN SAT	9.9 ± 0.4
PENN function	59.0 ± 1.7
PENN total	98.4 ± 2.4
Shoulder External Rotation (°)	101.7 ± 14.3
Shoulder Internal Rotation (°)	50.8 ± 9.0
Shoulder Abduction (°)	152.0 ± 9.3
Shoulder Flexion (°)	160.4 ± 6.6
Shoulder External Rotation Strength (lbs.)	19.9 ± 4.7
Shoulder Internal Rotation Strength (lbs.)	19.3 ± 7.5
Shoulder Abduction Strength (lbs.)	21.3 ± 8.0

Table 1. Participant Demographic Data

Participant information including age, weight, height, PENN scores, shoulder ROM measures, and shoulder strength measures.

IRB Consideration

This investigation was approved by the Marshall IRB (IRBNet #1399964) (Appendix A).

All participants provided written informed consent prior to the start of data collection.

Inclusion Criteria

1. Marshall University student
2. Between the ages of 18 and 29

Exclusion Criteria

1. Any history of shoulder injury
2. Any current arm or shoulder pain

Pilot Study

A pilot study with 10 participants was conducted to practice the technique, to capture images of the supraspinatus while stabilizing the participant's shoulder and collecting force data, and to determine parameters of the Ncorr analysis software, particularly, the subset radius and strain radius parameters. The subset radius determines the size of the area around a particular speckle that is compared to that speckle. The strain radius determines the size of the area around a particular speckle that is used to determine strain. From the pilot work, it was determined that the subset radius and strain radius should both be 20 pixels. Twenty (20) was selected for both the subset radius and the strain radius, because 20 gave us results that were consistent and minimized processing time. Values that were larger or smaller lead to results that were either inconsistent or a much longer time to process. All other parameters were kept at the current or recommended settings.

Instrumentation

A Mindray M5 Ultrasound scanner with variable frequency 5cm sound head (Shenzhen Mindray Bio-Medical Electronics Co LTD, Shenzhen, China) was used for ultrasound image collection. MATLAB R2017b (The MathWorks, Inc., Natick, MA) and Ncorr (Ncorr, Blaber and Antoniou, Georgia Institute of Technology) (Blaber et al., 2015) were used for speckle

tracking analysis. Measurements of force will be made using a handheld dynamometer (microFET2, Hoggan Scientific LLC, Salt Lake City, UT). All statistical calculations will be performed using SPSS 24.0 (IBM, Chicago, IL).

Protocol

A repeated measures design was used to test the alternative hypothesis. Longitudinal ultrasound images of the supraspinatus tendon (Figure 1) were collected during 5 maximal isometric arm abduction contractions. Scapular and humeral motion was controlled during the maximal abduction contraction using external stabilization techniques (Figures 5 and 6). Ultrasound cine loops files were exported from the ultrasound unit and saved as AVI files. AVI files were imported into the Ncorr software for speckle tracking analysis. Strain measurements were made at the bursal side (top), mid-substance, and joint side (bottom) of the widest visualized point of the supraspinatus tendon. Strain was measured in an axis parallel to, and perpendicular to the long axis of the tendon (Figure 2). Strain parallel to the long axis of the tendon will be referred to as longitudinal strain. Strain orthogonal to the long axis of the tendon will be referred to as axial strain.

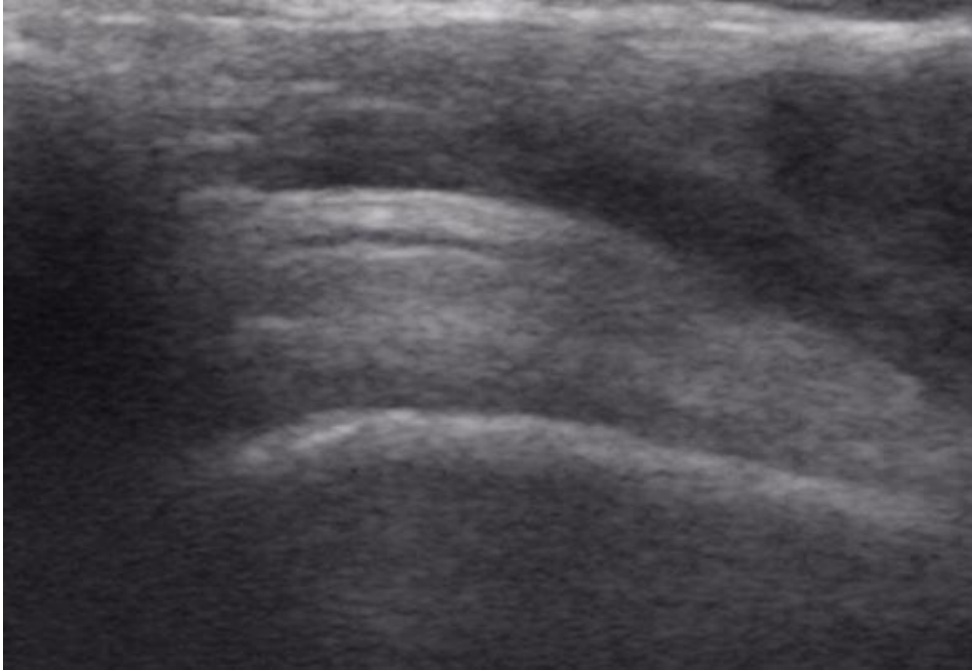


Figure 1. Longitudinal Ultrasound Image of Supraspinatus tendon

A greyscale ultrasound image of the right-side supraspinatus tendon. The top of the image is where the ultrasound transducer is placed.

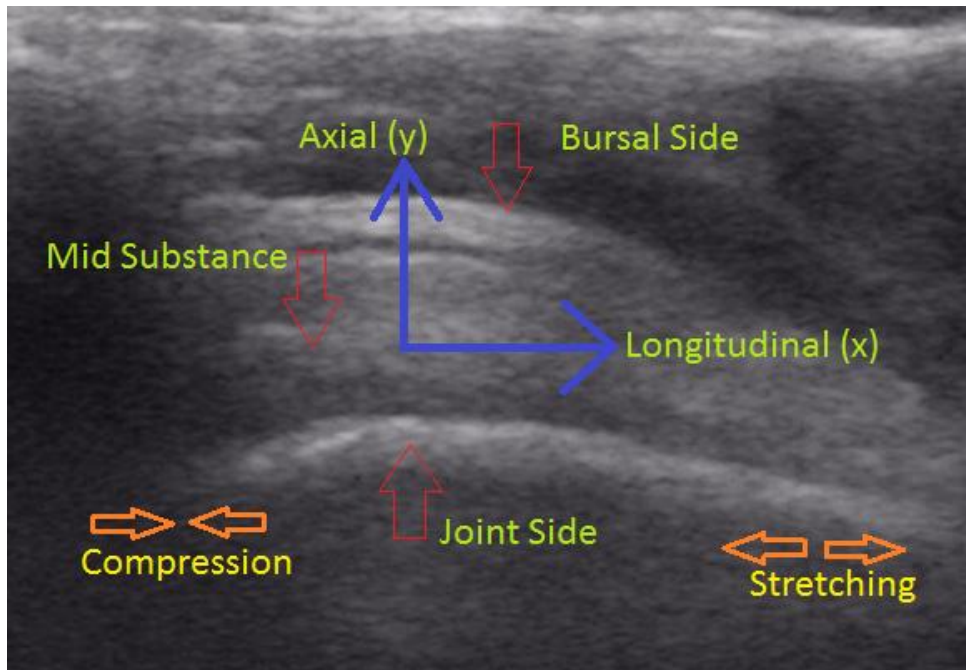


Figure 2. Strain Direction and Tendon Position Labels

The two dark blue arrows represent the direction in which the longitudinal (x) and axial (y) strains occur. The longitudinal strain is along the length of the tendon while the axial strain is orthogonal to the longitudinal strain, vertically. Positive strain values represent expansion or stretching while negative strain values represent compression or shrinking. The arrows do not represent positive or negative directions, since strain is not a vector. The inward, bottom left, and outward, bottom right, facing orange arrows represent compression and stretching, respectively.

Procedures

Demographics

Demographic information including height, weight, sex, current age, arm dominance, and affected arm was collected. Demographics were collected for future comparisons, such as strain differences versus BMI, sex, age, or arm dominance.

Self-Reported Outcome Measures

The PENN is a 25-item questionnaire that accesses the participant's level of pain, function and level and satisfaction with the function of their shoulder. The total score on the PENN is the combination of the pain, satisfaction and function scores, the PENN is scored 0-100 with a score of 100 equating to no pain, no disability and maximum satisfaction with the function of their shoulder. The PENN pain score is a maximum of 30, the PENN satisfaction score is a maximum of 10, and the PENN function score is a maximum of 60. These questionnaires have been found to be valid and reliable, as well as useful tools in tracking the progress of therapeutic exercise treatment (Leggin et al., 2006). The PENN was used to exclude participants with high levels of pain and/or low levels of function of their right shoulder.

Physical Examination

Physical impairments of the shoulder were determined through a standard clinical examination of the shoulder. This examination included range of motion (active and passive), assessment of strength of the shoulder musculature, assessment of posture and special test designed to elicit symptoms of specific shoulder pathologies. Range of motion measurements were performed; specifically, shoulder flexion, extension, abduction, internal and external rotation, and horizontal adduction were measured with a digital angle gauge.

Manual Muscle Strength

Assessment of shoulder girdle muscle strength was performed using techniques described by Kendall, McCreary, and Provance (1993). Strength was determined for the following muscles of the shoulder; serratus anterior, lower, and middle trapezium, and the following shoulder motion; external rotation, internal rotation, and shoulder adduction. Muscle strength was measured using a microFET2 handheld dynamometer (Hoggan Scientific LLC, Salt Lake City,

UT). Force was recorded to the nearest tenth of a pound. Each measurement was made twice; a minimum 60 second rest was given between each measurement.

External rotation

External rotation strength was assessed by having the participant stand upright with their arm hanging in a relaxed slightly abducted position with the elbow flexed to 90°. The examiner stood to the side of the participant with one hand stabilizing the participant's elbow; the examiner grasped the participant's wrist with their other hand. The participant was instructed to externally rotate their shoulder. The examiner resisted their motion (Kendall et al., 1993).

Internal rotation

Internal rotation strength was assessed by having the participant stand upright with their arm hanging in a relaxed slightly abducted position with their elbow flexed to 90°. The examiner stood to the side of the participant with one hand stabilizing the participant's elbow. The examiner grasped the participant's wrist with their other hand. The participant was instructed to internally rotate their shoulder. The examiner resisted their motion (Kendall et al., 1993).

Shoulder abduction

Shoulder abduction strength was assessed by having the participant stand with their arm at their side. The examiner stood in front of the participant, grasped the participant's wrist, and passively abducted the participant's arm. The examiner placed their other hand at the level of the participant's elbow. The participant was instructed to abduct their arm. The examiner applied a force that resisted the participant's motion (Kendall et al., 1993).

Shoulder Clinical Tests

Special tests to evaluate for clinical signs of shoulder pathology were used. The glenohumeral joint was assessed for anterior, posterior, and multidirectional instability. Specifically, the load shift, anterior release, apprehension relocation and sulcus tests were performed. Scapular motion was assessed for signs of scapular dyskinesis during arm elevation in the plane of the scapula. The procedure for assessing scapular dyskinesis has been described by McClure, Tate, Kareha, Irwin, and Zlupko (2009) and Tate, McClure, Kareha, Irwin, and Barbe (2009). Signs of rotator cuff impingement and tear were assessed using the Neer, Kennedy-Hawkins, and painful arch tests (Michener, Walsworth, Doukas, & Murphy, 2009).

Glenohumeral Stability

Apprehension Relocation

The apprehension relocation test was performed by having the participant lay supine with their arm abducted to 90° with the elbow flexed to 90°. From this position the examiner passively externally rotated the participant's arm. A positive was recorded if the patient expressed a look of apprehension or alarm on their face (C. S. Neer, 1985; Speer, Hannafin, Altchek, & Warren, 1994; Warner, Micheli, Arslanian, Kennedy, & Kennedy, 1990).

Anterior Release

The anterior release test was performed in the same position as the apprehension relocation test. From this position the relocation force was removed. A positive test was recorded if the participant experienced pain or apprehension when the relocation force was removed (C. S. Neer, 1985; Speer et al., 1994; Warner et al., 1990).

Sulcus Sign

The sulcus sign test was performed by having the participant sit upright with the participant's arm in a relaxed position at their side. The examiner placed one hand on the participant's shoulder over the acromioclavicular joint; with their other hand the examiner grasped the participant just proximal to the elbow. The examiner applied a traction force to the shoulder. A positive test was recorded if a sulcus developed over the glenohumeral joint lateral to the acromioclavicular joint (C. S. Neer, 1985; Speer et al., 1994; Warner et al., 1990).

Rotator Cuff Pathology

Painful Arc Test

The painful arc test was performed by having the participant actively elevate their arm in the plane of the scapula through a complete range of motion. A positive test was recorded if the participant complained of pain in the 60° - 120° arc of motion (Park, Yokota, Gill, El Rassi, & McFarland, 2005).

Neer Test

The Neer test was performed by having the participant internally rotating their arm; from this position the participant elevated their arm in the sagittal plane while the examiner stabilized the scapula. A positive test was recorded if the participant experienced pain at the end range of motion (Neer, 1983).

Kennedy Hawkins Test

The Kennedy Hawkins test was performed by having the participant elevate their arm to 90 degrees in the sagittal plane; the arm was then passively internally rotated. A positive test was recorded if the participant experienced pain at the end range of motion (Michener et al., 2009; Park et al., 2005).

Ultrasound Imaging

Phase I Standard Ultrasound Assessment

A diagnostic ultrasound unit, (Mindray M5; Mindray Ltd., National Ultrasound, Inc., Duluth, GA USA) with an adjustable 6.0-12.0 MHz frequency linear array transducer was used to capture all images. A comprehensive ultrasound imaging evaluation of the shoulder was performed, which included evaluating the shoulder for tendon or muscle tears, tendinosis, muscle atrophy, joint and bursal effusions, calcified tendon, impingement syndrome, as described by Jacobson (Jacobson, 2011). In addition to the comprehensive examination a targeted examination of the structures of the rotator cuff were imaged. This procedure imaged the structures that are most common sites of shoulder pain and will allow for the assessment of the structures involved in the individual participant. Anatomical structures imaged in order of evaluation as recommended by Jacobson (2011) are:

1. The supraspinatus tendon
2. Acromion humeral distance,
3. The cross-sectional area of the supraspinatus muscle.
4. Dynamic evaluation, rotator cuff impingement,

For measurements of tendon thickness, ultrasound images were taken in the standard I and II views (transverse and longitudinal views) as described by Teefey, Middleton, and Yamaguchi (1999) for best visualization of the supraspinatus tendons. The participant was seated with the hand of the arm to be tested positioned on their iliac crest-hip. The elbow was directed posteriorly.

Phase 2 Ultrasound for Speckle Tracking

The participant was seated with their shoulder and upper arm exposed. The participant was asked to extend their arm fully downward to their side while turning their hand so that their thumb was pointed towards their body. For measurements of strain, the ultrasound transducer was placed flat on the most anterior aspect of the lateral acromion (Figure 3). The linear array transducer frequency was set to 10 MHz. A handheld force transducer was held against the participant's wrist and the participant's scapula was stabilized by placing a fist at the inferior angle of the participant's right scapula and anterior portions of the shoulder in place (Figure 4 and Figure 5). The ultrasound probe, force transducer, and scapula stabilization set up can be seen in Figure 6. The force transducer prevented the participant from being able to abduct their arm so that the maximal abduction was isometric. The force transducer collected force data from when the participant started contracting to when the participant stopped contracting. The participant's shoulder was stabilized to prevent movement of the scapula, which, with preventing the participant from abducting, would prevent the origin and insertion of the supraspinatus tendon from moving during the contraction, an isometric contraction. Stabilizing the participant's scapula helped to prevent the ultrasound probe or the participant's shoulder from moving. Any movement of the ultrasound probe or the participant's shoulder could have led to the ultrasound image moving out of frame of the supraspinatus tendon. Diagnostic ultrasound video collection started approximately one second before participants were asked to start arm elevation, and video collection ended after participants reached maximal contraction.



Figure 3. Data collection with Ultrasound Transducer (Photo by Dr. Mark Timmons)
The ultrasound transducer is placed flat on the most anterior aspect of the lateral acromion in line with the tendon.



Figure 4. Force Transducer Placement, Wrist View (Photo by Dr. Mark Timmons)
A handheld force transducer was held against the participant's wrist while the participant's arm was fully extended and internally rotated.



Figure 5. Scapula Stabilization, Side View (Photo by Dr. Mark Timmons)

The right scapula of the participant was stabilized by placing a fist against the inferior angle and placing a hand against the coracoid process.



Figure 6. Data Collection Setup (Photo by Dr. Mark Timmons)

Ultrasound transducer placed flat on the most anterior aspect of the lateral acromion, force transducer placed against participant's wrist, and participant's scapula being stabilized.

Speckle Tracking

Ultrasound AVI files that were obtained, as described in the previous section, were imported to be analyzed by Ncorr in MATLAB. Two frames from the files were extracted, the second, reference image, and sixth, current image, frames. The reference image, which sets the initial length or dimension of all speckles, is the frame of the ultrasound video that is the starting point of the movement. The current image, which sets the current length or dimension of all speckles, is the frame, or set of frames, of the ultrasound video that is the point at which strain is

determined. The Ncorr system was opened and the reference image and current images were loaded by clicking on file and selecting the frames wanted (Figure 7).

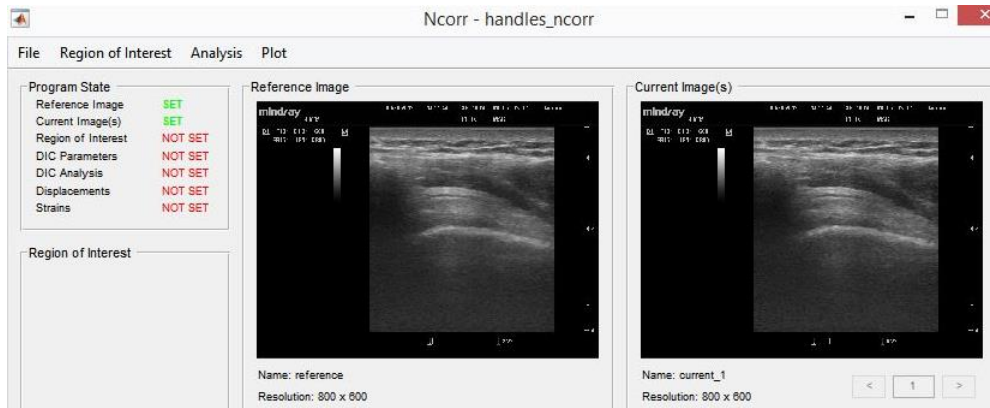


Figure 7. Reference and Current Images Set

The reference image, on the left, and the current image, on the right, are set into the Ncorr window.

The region of interest was set on the reference image with a preview on the current image by clicking on “Region of Interest” on the Ncorr window (Figures 8 and 9). The region of interest is the area of the ultrasound image that will be processed to determine strain. The region of interest is an N-sided polygon.

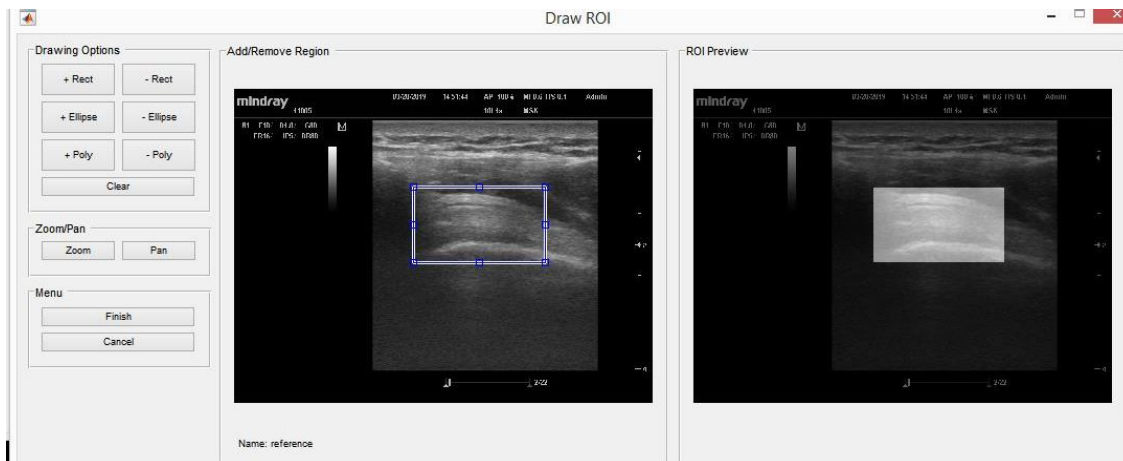


Figure 8. Region of Interest

The region of interest, the blue rectangle on the left image and the opaque box on the right image, is being set over the ultrasound image of the supraspinatus tendon.

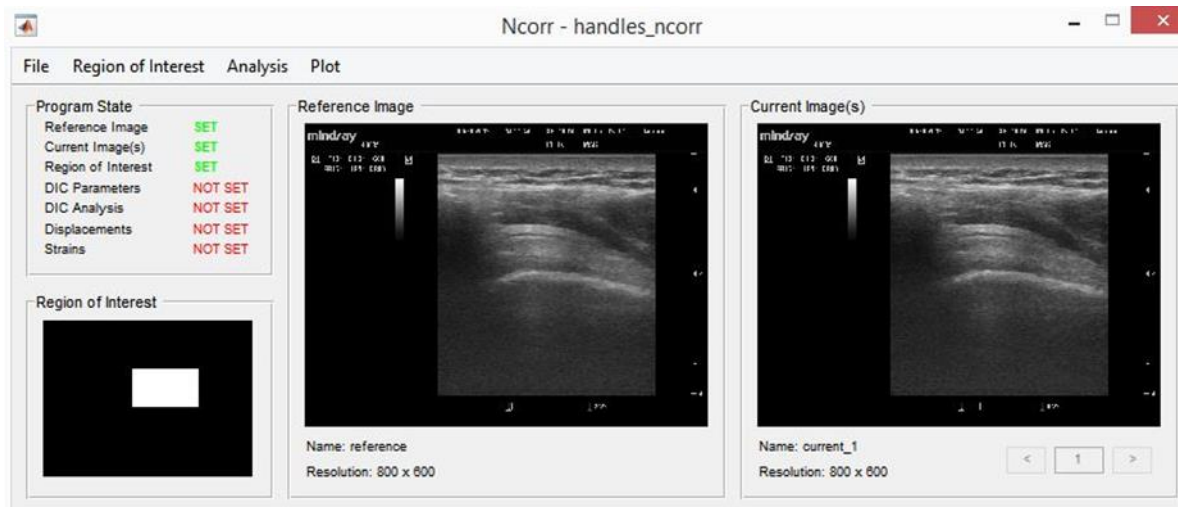


Figure 9. After Region of Interest is Set

The region of interest has been set, as can be seen by the green “set” on the left side of the figure.

The Digital image correlation (DIC) parameters were set, by clicking on “Analysis” and then “DIC Parameters,” to the pre-determined settings of subset radius at 20, subset spacing at 1, and step analysis enabled (Figures 10 and 11). The DIC parameters are the digital image correlation parameters which determine how the region of interest previously selected is processed. Digital image correlation compares a reference image with a current image by checking speckles, or small subset areas, in the region of interest of the reference image to determine where that region may have moved to in the current image. The speckles have an initial length or dimension, which will change from the reference image to current image. This change, which is determined in the DIC process, is what is calculated as strain.

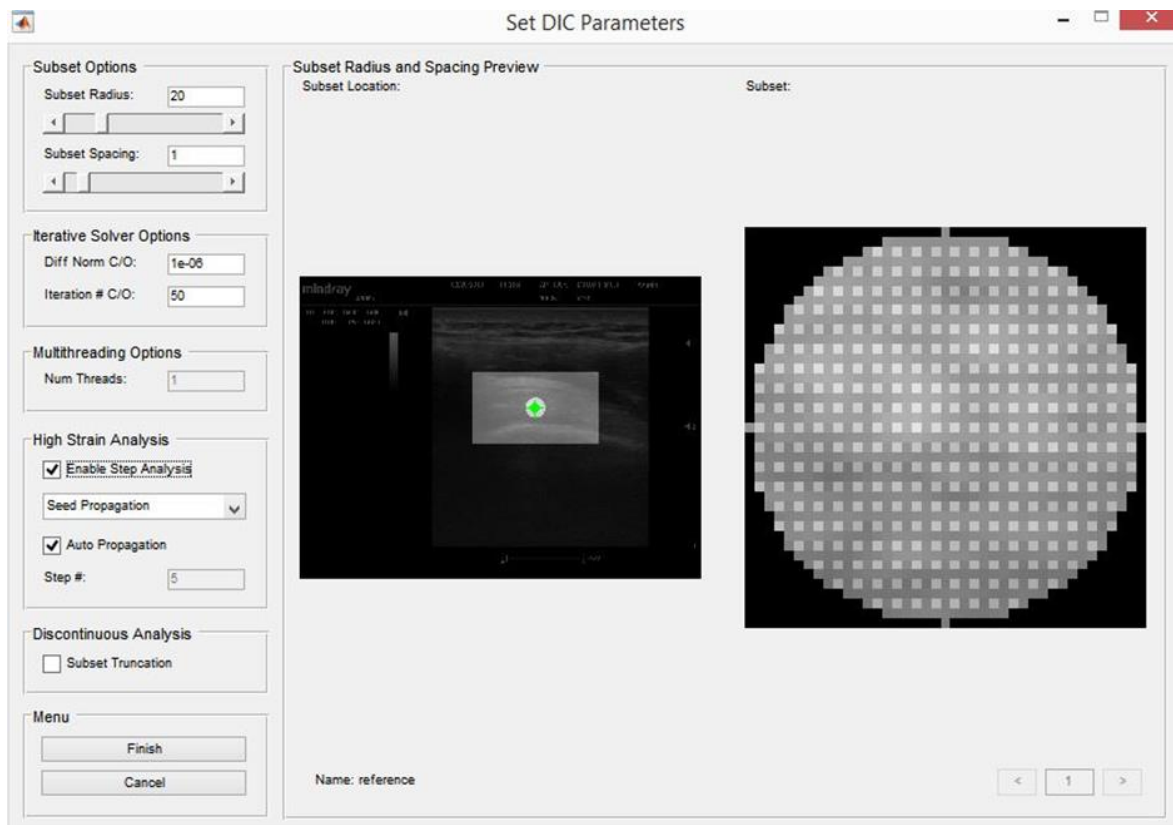


Figure 10. DIC Parameters

The DIC parameters, which can be seen on the left side of the figure, are set to appropriate values. The image on the right side shows an example of the subset radius and spacing of the circled area on the left side ultrasound image.

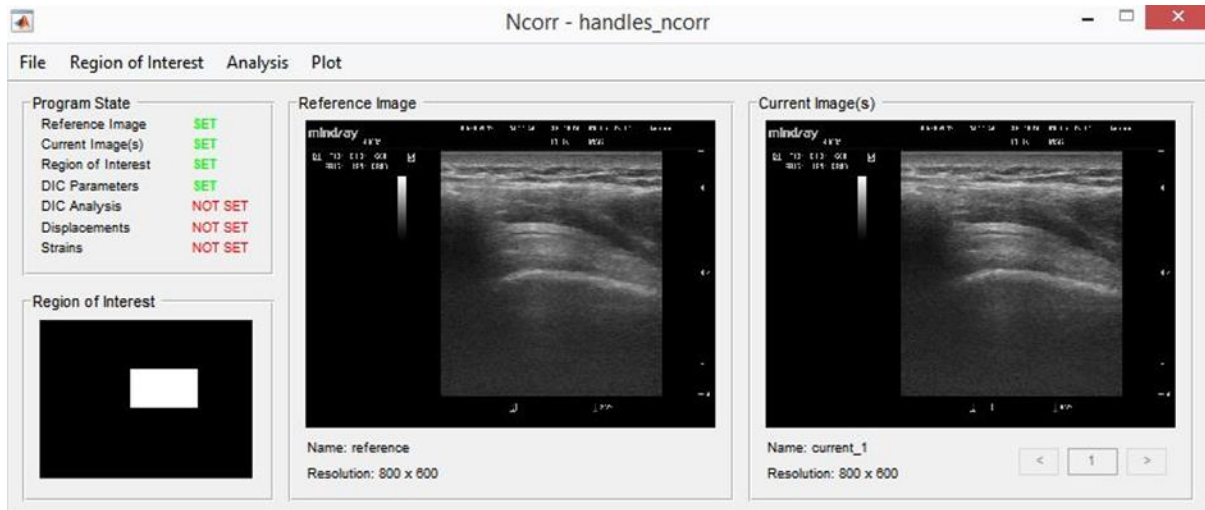


Figure 11. After DIC Parameters are Set

The DIC Parameters have been set, as can be seen by the green “set” on the left side of the figure.

Digital Image Correlation (DIC) analysis was performed by clicking on “Analysis” and then “DIC Analysis” (Ab Ghani et al., 2016). The DIC analysis requires setting a seed, which is a test case of the DIC analysis that lets the observer determine if the DIC analysis will work appropriately. After the seed is set and the observer determines the analysis will be appropriate, the observer completes the analysis. An example of the DIC analysis not working appropriately would either be an error message that the seed placement failed, which means that the DIC analysis cannot be performed for some internal reason of the Ncorr software, or that the seed moved well beyond the bounds of the tendon or region of interest, which is not necessarily physiologically possible. In Figure 12, it can see that the placed seed is a green dot placed by the observer within the region of interest. In Figure 13, it can see a preview of where the seed would move, from the reference image to the current image, because of the DIC analysis. This figure lets us see where the DIC analysis determined the subset region on the reference image is most correlated to on the current image, and the figure lets us see what the zoomed in regions look like to help determine appropriateness. In Figure 14, it can see that the DIC analysis is completed.

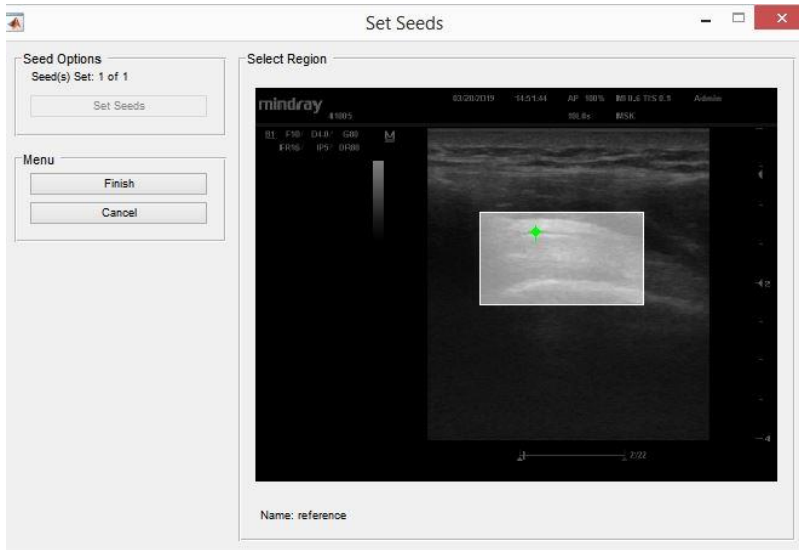


Figure 12. Setting Seed

The seed is placed within the region of interest on the reference image, which will then be used to test the DIC analysis.

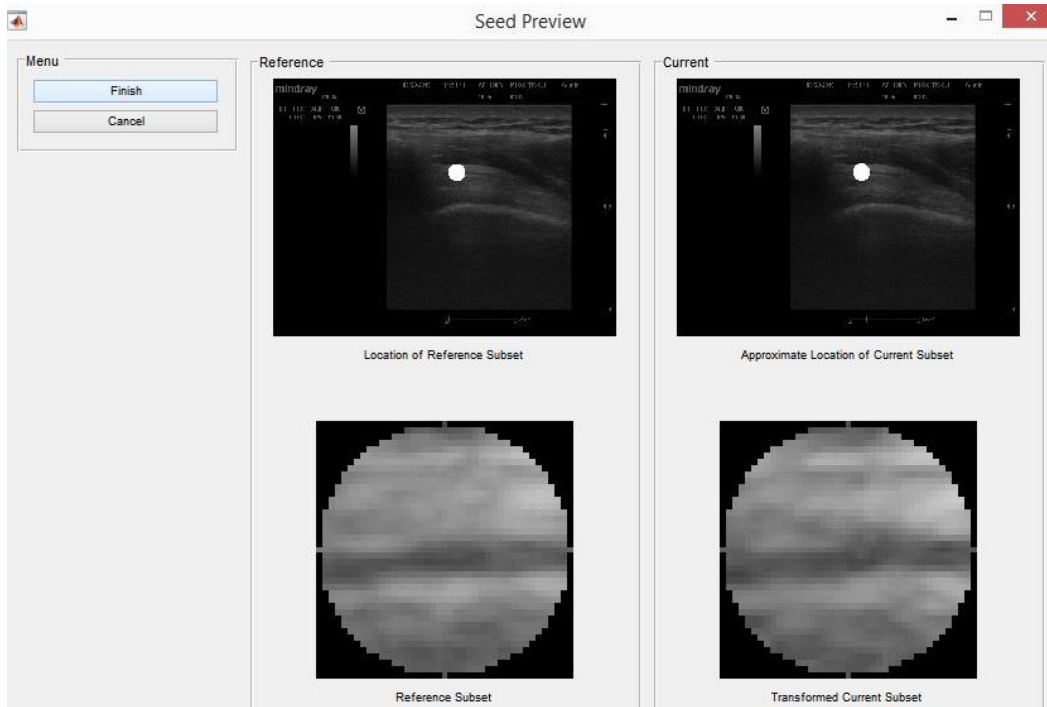


Figure 13. Seed Preview, After Setting Seed

The top left image shows the seed placement area on the reference image, and the bottom left image shows a zoom in of the same area. The top right image shows the seed placement area on the current image, and the bottom right image shows a zoom in of the same area.

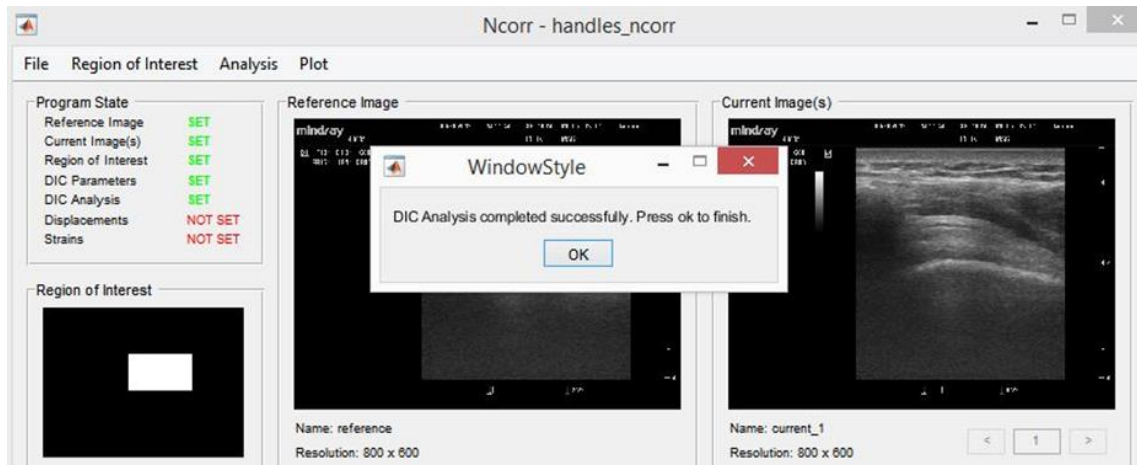


Figure 14. After DIC Analysis is Complete

The DIC Analysis has been completed, as can be seen by the green “set” on the left side of the figure.

The displacements were then formatted by clicking on “Analysis” and “Format Displacements” (Figures 15 and 16). Displacements, or the change in position, were determined by the change in the location of speckles, or subset areas, from the reference image to the current image. All options were kept to the base setting for Ncorr. The correlation coefficient cutoff was maximized, which is the base setting, so that the area determined displacements inside the region of interest was maximized.

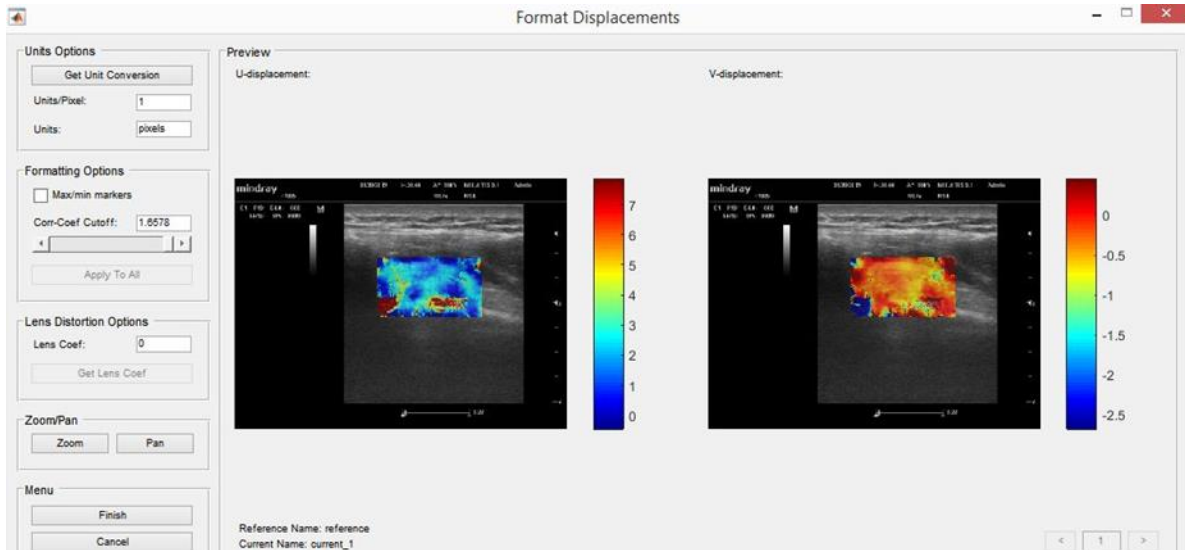


Figure 15. Formatting Displacements

The displacements are being formatted to the base setting for Ncorr, which includes setting the correlation coefficient cutoff to the maximum value.

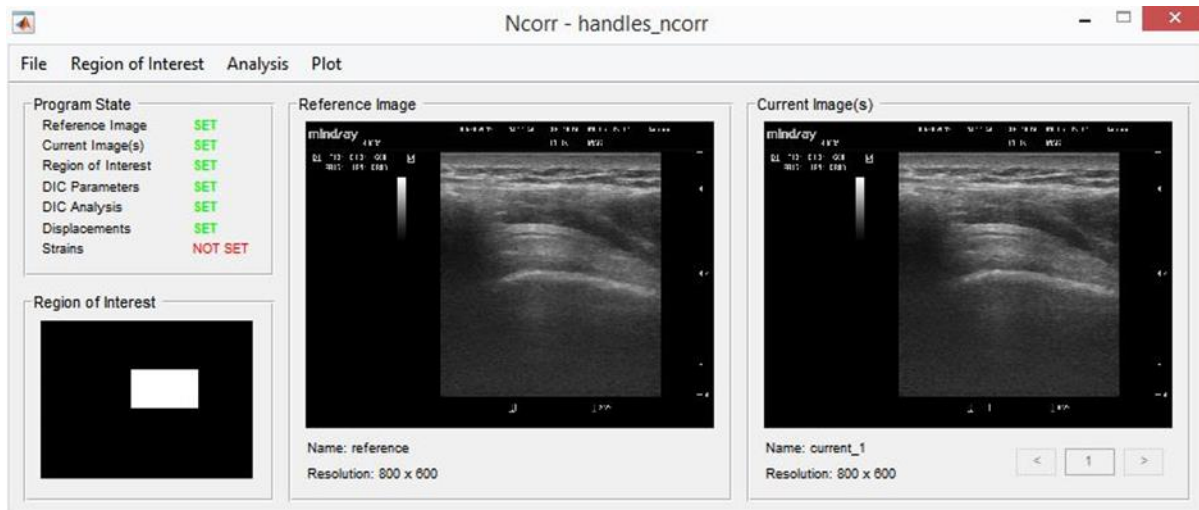


Figure 16. After Displacements are Formatted

The Displacements have been formatted, as can be seen by the green “set” on the left side of the figure.

Strain analysis was then performed by clicking “Analysis” and “Strain Analysis” (Figures 17 and 18). The strain radius was set to 20, which was determined to be the most appropriate value from the pilot study.

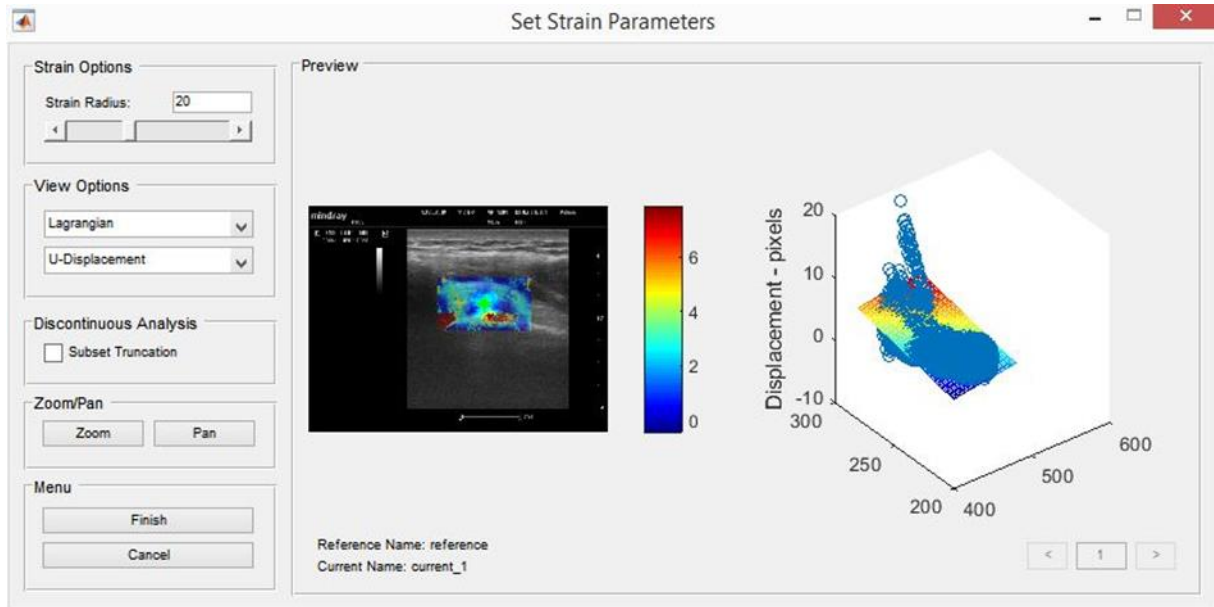


Figure 17. Setting Strain Parameters

The strain parameter of strain radius is set to 20, which was determined in the pilot study to be the value that best determines to most strain without taking too much time or introducing too much error.

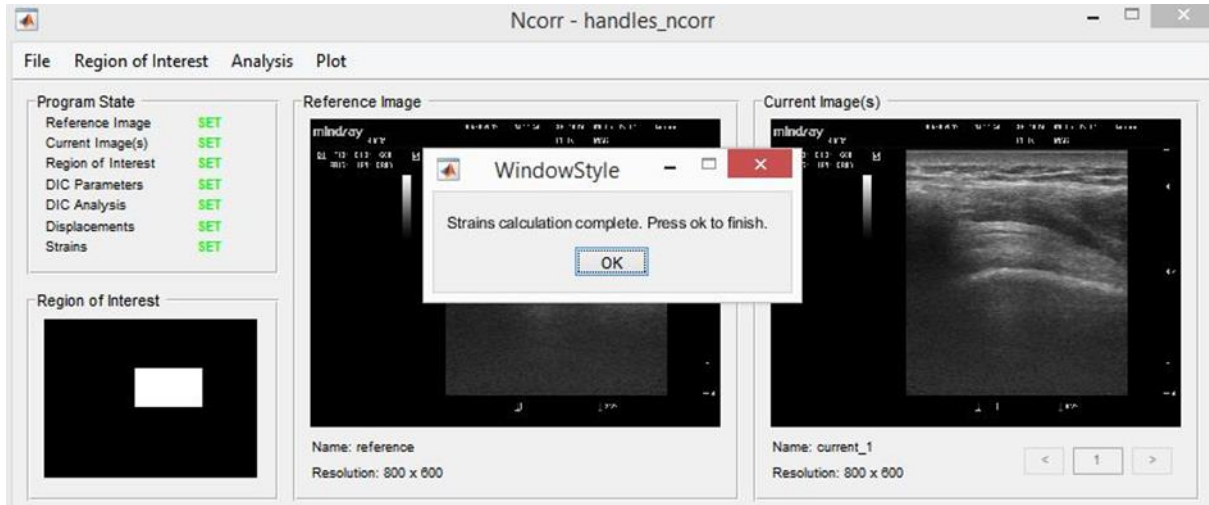


Figure 18. After Strains are Calculated

The Strains have been calculated as can be seen by the green “set” on the left side of the figure.

The longitudinal strain, strain horizontal relative to the image, and axial strain, strain vertical relative to the image, were then plotted for each of the current images by clicking on “Plot” (Figures 19 and 20). The longitudinal and axial strains are not necessarily the exact same as the horizontal and vertical strain relative to the image, since the image or tendon may not line up perfectly. The longitudinal strain, found in Figure 19, is strain horizontal, relative to the figure that lines up with fibers of the tendon from muscle to insertion. The axial strain, found in Figure 20, is strain vertical, relative to the figure that is to be orthogonal to the longitudinal strain. A compass, two arrows showing the directions for longitudinal and axial, can be seen at the top left of the plots in Figures 19 and 20.

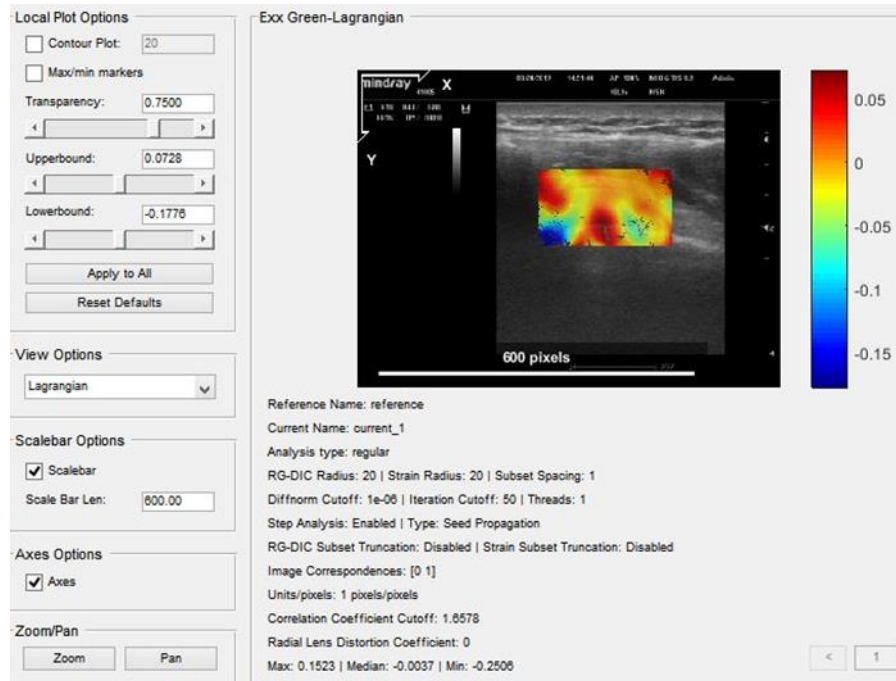


Figure 19. Longitudinal (x) Direction Strain Map

The colored in rectangle, which is the region of interest, shows the magnitudes of the longitudinal direction strain. A color key is shown to the right of the image. Plot options are available on the left.

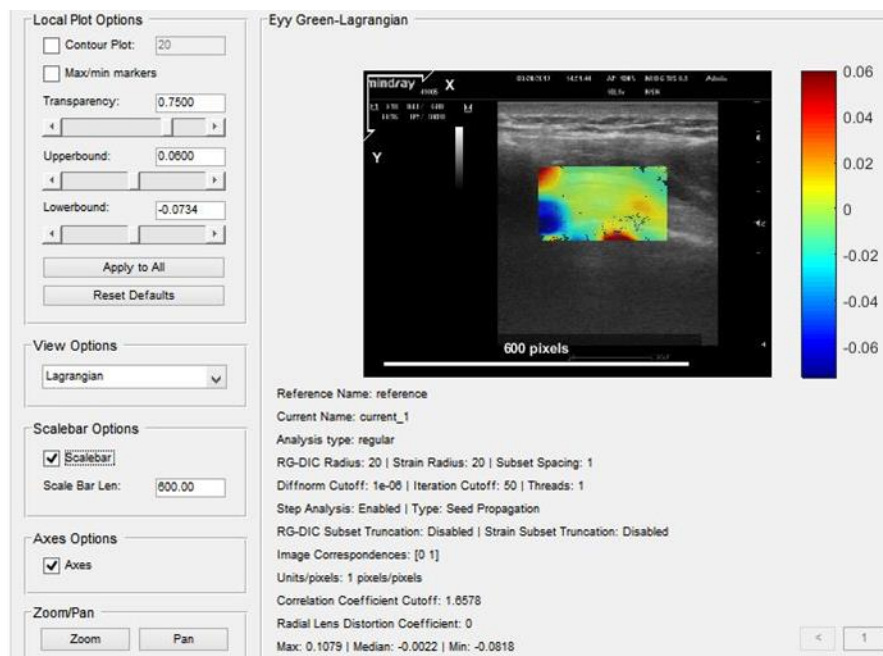


Figure 20. Axial Direction Strain Map

The colored in rectangle, which is the region of interest, shows the magnitudes of the axial direction strain. A color key is shown to the right of the image. Plot options are available on the left.

Longitudinal and axial strain values and coordinates at the bursal side, mid-substance, and the joint side of the thickest portion of the supraspinatus tendon in the region of interest were recorded. Positive values of strain mean there is stretching of the tissue. Negative values of strain mean there is compression of the tissue.

Statistical Analysis

The interclass correlation coefficient (ICC) was determined using the strain measures from the 3 location in the supraspinatus tendon during the 5 maximal isometric contractions, in order to determine the inter image consistency of the strain measures. The higher the consistency, or ICC, the higher the reliability. Strain was measured using image 1 twice, ICCs were calculated using the repeated strain measures in order to determine the Intra image

consistency of strain measurements. Intraclass correlation coefficients [ICC(2-way random)] were used to determine the inter-rater reliability of the all strain measurements (Shrout & Fleiss, 1979). ICC values were considered very good for values 0.81-1.00, good for 0.61-0.80, moderate for 0.41-0.60, fair for 0.21-0.40, and poor for values below 0.20 (Poiraudau et al., 2001). The standard error of the measure (SEM) and minimal detectable change (MDC) for the strain measures were calculated. Measurement error was calculated with the standard error of measure $SEM = \text{standard deviation} \times [\sqrt{(1-ICC)}]$, which estimates the error about a single measure of a variable. The lower the error, or MDC, the higher the precision. The MDC represents the error when a measure is taken twice (change over time), and was calculated by multiplying the SEM by the $\sqrt{2}$ (Stratford, 2004; Weir, 2005). All statistical calculations were performed using SPSS 24.0 (IBM, Chicago, IL). Systematic error was assessed using Bland-Altman plots. Bland-Altman plots were created for differences between the 1st and 2nd images and between the 1st and 5th images. These were selected to see the changes between measurements taken consecutively and measurements taken with multiple measurement between each other. The x-axis of the Bland-Altman plots represents the mean of the first and second images. The y-axis of the Bland-Altman plots represents the difference between the first and second images (i.e. strain of image 1 minus strain of image 2). Student t-tests were also conducted for each of the Bland-Altman plots.

CHAPTER 4

RESULTS

The purpose of this study was to examine the reliability of speckle tracking to measure supraspinatus tendon strain during an isometric contraction with ultrasound speckle tracking. Participant measures of the PENN test, range of motions (ROM), and manual muscle strength are reported to show participants were without pain or impairment. The consistency of strain measures along with the measurement error for intra and inter image strain measurements are reported. Bland-Altman plots for both the intra- and inter-image measures are provided in order to explore systematic measurement error.

Intra Images

Four participants were excluded from the intra image testing, because the images were not able to be processed in Ncorr due to an error of seed placement. Values for the longitudinal direction strain, strain horizontal relative to the image, and axial direction strain, strain vertical relative to the image, are found in Table 2. Mean strain (%), ICC, 95% confidence interval for the SEM and MDC are presented to support the reliability and precision of the strain measures. The mean longitudinal direction strains across the imaged tendon locations ranged from -2.12 to 1.791%. The ICC of the longitudinal direction strain across the imaged tendon locations ranged between 0.982 and 0.992. The SEM at 95% confidence interval of the longitudinal direction strain across the imaged tendon locations ranged from 0.319% to 0.327%. The MDC at 95% confidence interval of the longitudinal direction strain across the imaged tendon locations ranged from 0.451% to 0.463%. The mean axial direction strains across the imaged tendon locations ranged from -1.129% to 0.342%. The ICC of the axial direction strain across the imaged tendon locations ranged from 0.984 to 0.99. The SEM at 95% confidence interval of the axial direction

strain ranged from 0.052% to 0.235%. The MDC at 95% confidence interval of the axial direction strain ranged from 0.074% to 0.333%. Values for the axial direction strain are found in Table 3.

Longitudinal	Bursal Side	Mid-substance	Joint side
Mean (%)	1.791	-1.405	-2.12
ICC	0.984	0.982	0.992
SEM 95% C. I. (%)	0.327	0.327	0.319
MDC 95% C. I. (%)	0.463	0.463	0.451

Table 2. Intra Image Results, Longitudinal-Strain

The values are for the longitudinal direction component. The values are comparisons within multiple strain measurements of the same image. For the bursal side, mid-substance, and joint side section of the widest portion of the tendon, the mean, as a percent change in length, ICC, SEM with 95% confidence interval and MDC with 95% confidence interval in the same units as the mean.

Axial	Bursal side	Mid-substance	Joint side
Mean (%)	-1.129	-0.035	0.342
ICC	0.988	0.984	0.990
SEM 95% C. I. (%)	0.235	0.052	0.184
MDC 95% C. I. (%)	0.333	0.074	0.261

Table 3. Intra Image Results, Axial-Strain

The values are for the axial direction component. The values are comparisons within multiple strain measurements of the same image. For the bursal side, mid-substance, and joint side section of the widest portion of the tendon, the mean, as a percent change in length, ICC, SEM with 95% confidence interval and MDC with 95% confidence interval in the same units as the mean.

Inter Images

Nine participants were excluded from the inter image testing. Eight participants' images were not able to be processed in Ncorr due to an error of seed placement. One participant had 4 images that were collected, which did not meet the required 5 images. Mean strain (%), ICC, SEM at 95% confidence (%), and MDC at 95% confidence (%) were calculated to determine the reliability and precision of repeated measures of longitudinal and axial direction strain between

multiple images of each participant’s shoulder (n = 32). The mean longitudinal direction strain across the tendon locations ranged from -1.941 to 1.765%. The ICC of the longitudinal direction strain across the imaged tendon locations ranged 0.957 to 0.970. The SEM at 95% confidence interval of the longitudinal direction strain across the imaged tendon locations ranged 0.436% to 0.631%. The MDC at 95% confidence interval of the longitudinal direction strain across the imaged tendon locations ranged 0.616% to 0.892%. Values for the longitudinal direction strain are found in Table 4. The mean of the axial direction strain across the imaged tendon locations ranged -1.053% to 0.387%. The ICC of the axial direction strain ranged 0.955 to 0.986. The SEM at 95% confidence interval of the axial direction strain across the imaged tendon locations ranged 0.045% to 0.449%. The MDC at 95% confidence interval of the axial direction strain across the imaged tendon locations ranged 0.064% to 0.635%. Values for the axial direction strain are found in Table 5.

Longitudinal	Bursal side	Mid-substance	Joint side
Mean (%)	1.765	-1.326	-1.941
ICC	0.957	0.970	0.962
SEM 95% C. I. (%)	0.575	0.436	0.631
MDC 95% C. I. (%)	0.813	0.616	0.892

Table 4. Inter Image Results, Longitudinal-Strain

The values are for the longitudinal direction component. The values are comparisons within multiple strain measurements of the same image. For the bursal side, mid-substance, and joint side section of the widest portion of the tendon, the mean, as a percent change in length, ICC, SEM with 95% confidence interval and MDC with 95% confidence interval in the same units as the mean.

Axial	Bursal side	Mid-substance	Joint side
Mean (%)	-1.053	-0.030	0.387
ICC	0.955	0.986	0.974
SEM 95% C. I. (%)	0.449	0.045	0.286
MDC 95% C. I. (%)	0.635	0.064	0.405

Table 5. Inter Image Results, Axial-Strain

The values are for the axial direction component. The values are comparisons within multiple strain measurements of the same image. For the bursal side, mid-substance, and joint side section of the widest portion of the tendon, the mean, as a percent change in length, ICC, SEM with 95% confidence interval and MDC with 95% confidence interval in the same units as the mean.

Bland-Altman Plots

Tables 6 and 7 show the results of student t-tests, which were performed to determine statistically significant differences between the values of strain, between the first and second images and the first and fifth images. Six participants were excluded for the comparisons between image 1 and image 2, because the images were not able to be processed in Ncorr due to an error of seed placement. Six participants were excluded for the comparisons between image 1 and image 5, because the images were not able to be processed in Ncorr due to an error of seed placement. One participant was excluded for the comparisons between image 1 and image 5, because that participant did not have a 5th image collected.

Bland-Altman plots (Figures 21-32) comparing the axial- and longitudinal-axis strains for the bursal side, mid-substance, and joint side of the first and second image and the first and fifth image for each participant. The longitudinal strain between images 1 and 5 of the bursal side Bland-Altman plot, Figure 30, reveals systematic error. The systematic error revealed in Figure 30 is a pattern of the difference in strain between images 1 and 5 increases as the mean strain between images 1 and 5 increases.

The t-tests analysis results found in Tables 6 and 7, performed to determine the statistically significant differences between the values of strain, show that the differences in axial strain at the joint side of the thickest portion of the tendon between images 1 and 5 is statistically significant ($p < 0.05$).

Images 1-2	Mean Difference (%)	Std. Deviation (%)	t	p-value
Axial Bursal side	0.00505	0.7158	0.042	0.967
Axial Mid-substance	-0.03246	0.13474	-1.445	0.157
Axial Joint side	-0.12349	0.61384	-1.207	0.236
Longitudinal Bursal side	0.11666	0.9668	0.724	0.474
Longitudinal Mid-substance	-0.10302	0.96239	-0.642	0.525
Longitudinal Joint side	-0.27331	1.027	-1.597	0.119

Table 6. T-tests of strain values between image 1 and image 2

Comparison between the measurements of the first and second images. The mean difference, standard deviation, test statistic value, and the p-value are presented for the axial and longitudinal directions of strain for the bursal side, mid-substance, and joint side region of the widest portion of the tendon. Mean difference and standard deviation are in percent change in length units.

Images 1-5	Mean Difference (%)	Std. Deviation (%)	t	p-value
Axial Bursal side	-0.07118	0.93557	-0.444	0.660
Axial Mid-substance	-0.01106	0.07675	-0.840	0.407
Axial Joint side	-0.27019	0.64367	-2.448	0.020
Longitudinal Bursal side	0.01398	0.88811	0.092	0.927
Longitudinal Mid-substance	-0.12354	0.68656	-1.049	0.302
Longitudinal Joint side	1.33680	8.31399	0.938	0.355

Table 7. T-tests of strain values between image 1 and image 5

Comparison between the measurements of the first and fifth images. The mean difference, standard deviation, test statistic value, and the p-value are presented for the axial and longitudinal directions of strain for the bursal side, mid-substance, and joint side region of the widest portion of the tendon. Mean difference and standard deviation are in percent change in length units.

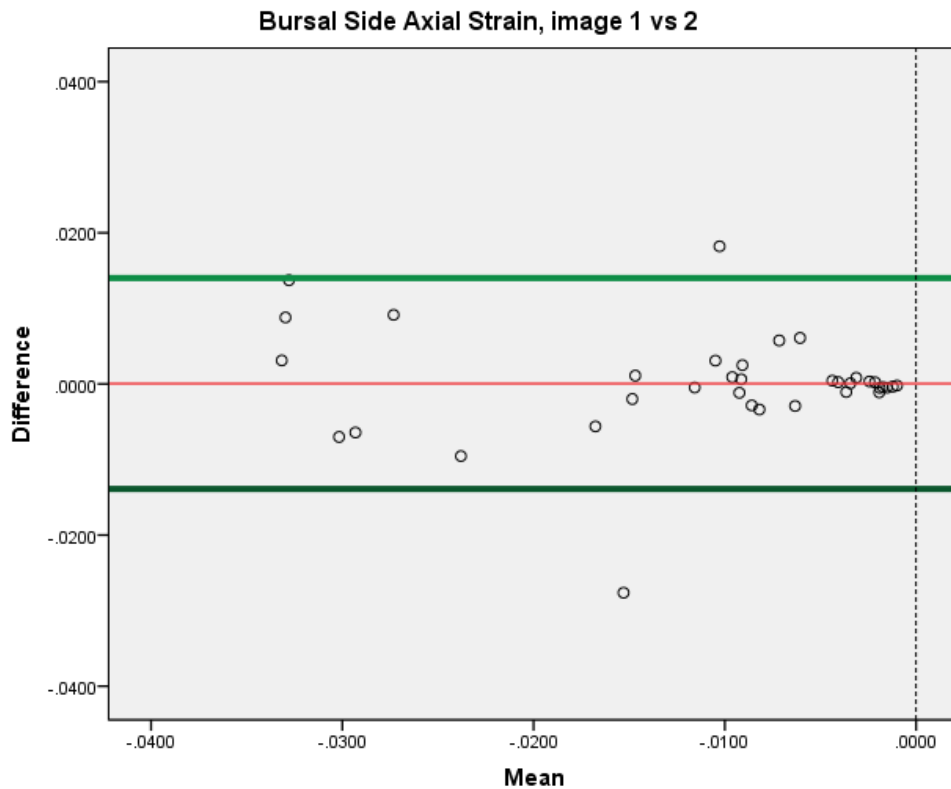


Figure 21. Bland-Altman of Bursal side Axial strains for Image 1 and Image 2

Bland-Altman plot of the Bursal Side Axial Strains between image 1 and image 2. The x axis, Mean, is the mean of the values of images 1 and 2. The y axis, Difference, is the difference between image 1 and image 2. The red horizontal line represents the mean of the differences, or the mean of the y axis values. The two green horizontal lines represent the mean of the differences plus or minus two standard deviations, or the 95% confidence interval of the mean difference. The dotted vertical line represents zero mean strain.

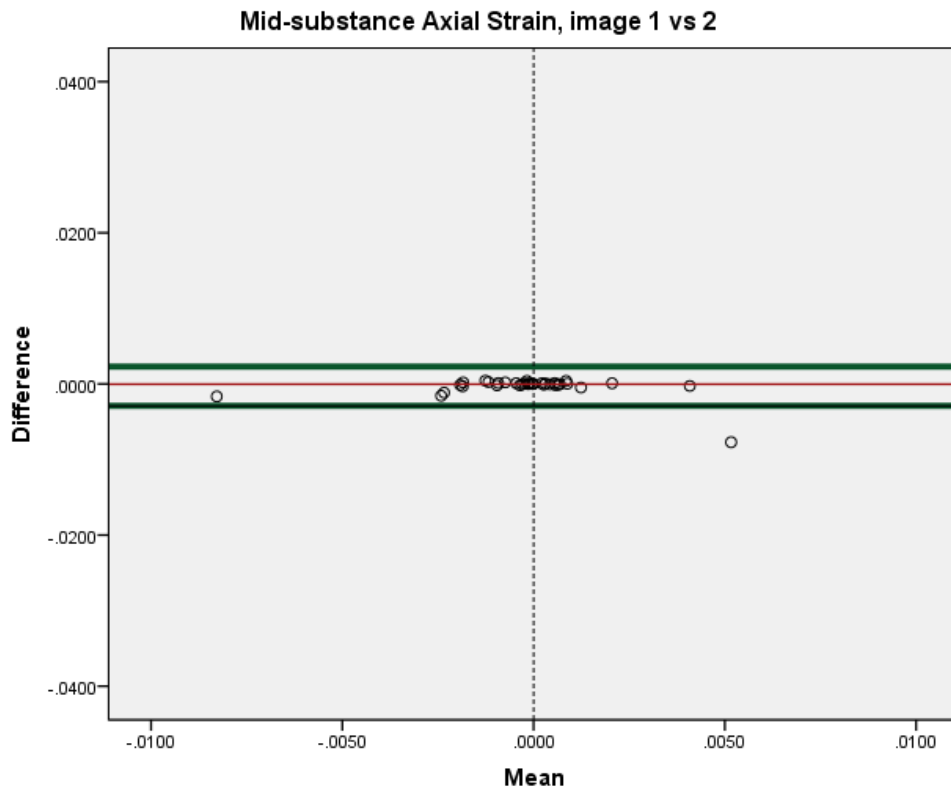


Figure 22. Bland-Altman of Mid-substance Axial strains for Image 1 and Image 2
 Bland-Altman plot of the Mid-substance Axial Strains between image 1 and image 2. The x axis, Mean, is the mean of the values of images 1 and 2. The y axis, Difference, is the difference between image 1 and image 2. The red horizontal line represents the mean of the differences, or the mean of the y axis values. The two green horizontal lines represent the mean of the differences plus or minus two standard deviations, or the 95% confidence interval of the mean difference. The dotted vertical line represents zero mean strain.

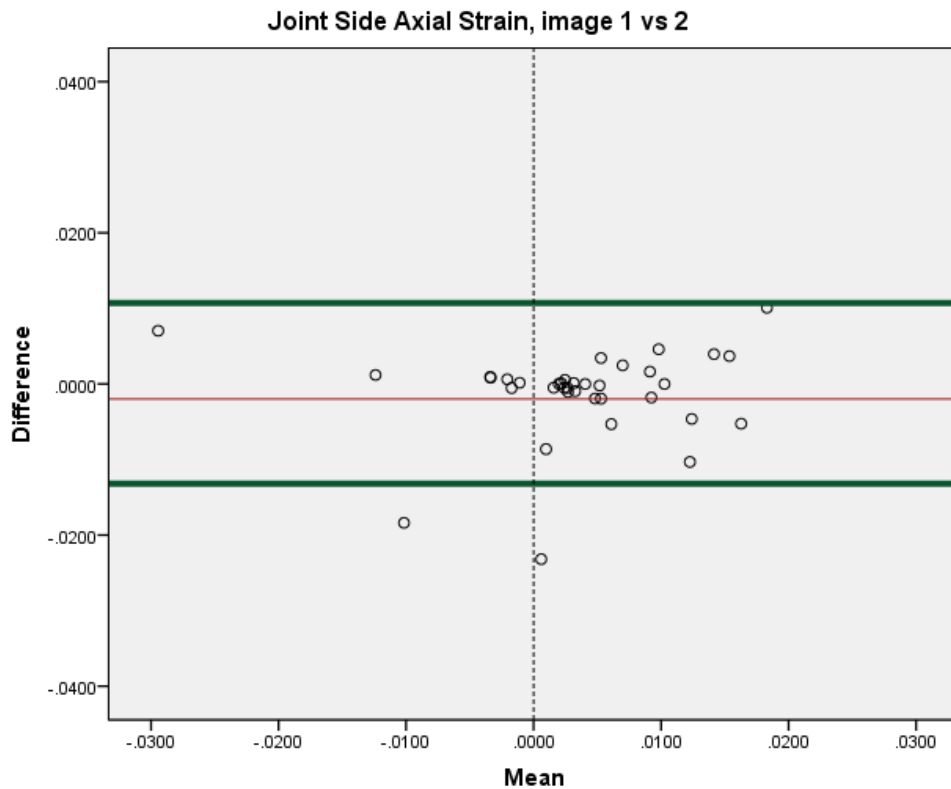


Figure 23. Bland-Altman of Joint side Axial strains for Image 1 and Image 2

Bland-Altman plot of the Joint Side Axial Strains between image 1 and image 2. The x axis, Mean, is the mean of the values of images 1 and 2. The y axis, Difference, is the difference between image 1 and image 2. The red horizontal line represents the mean of the differences, or the mean of the y axis values. The two green horizontal lines represent the mean of the differences plus or minus two standard deviations, or the 95% confidence interval of the mean difference. The dotted vertical line represents zero mean strain.

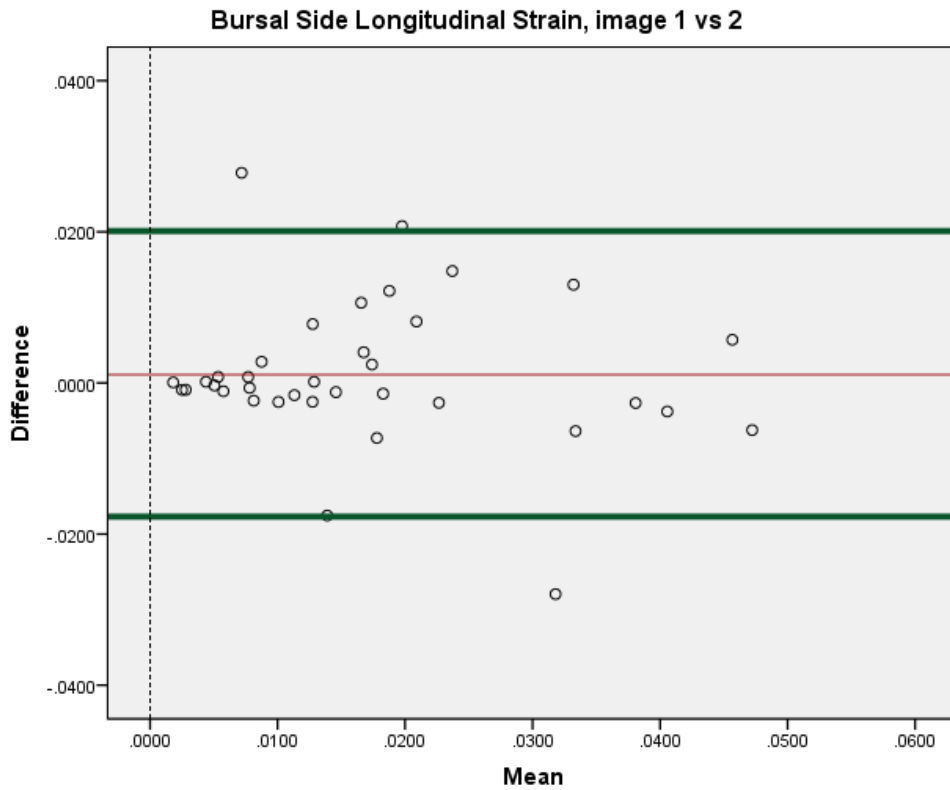


Figure 24. Bland-Altman of Bursal side Longitudinal strains for Image 1 and Image 2

Bland-Altman plot of the Bursal Side Longitudinal Strains between image 1 and image 2. The x axis, Mean, is the mean of the values of images 1 and 2. The y axis, Difference, is the difference between image 1 and image 2. The red horizontal line represents the mean of the differences, or the mean of the y axis values. The two green horizontal lines represent the mean of the differences plus or minus two standard deviations, or the 95% confidence interval of the mean difference. The dotted vertical line represents zero mean strain.

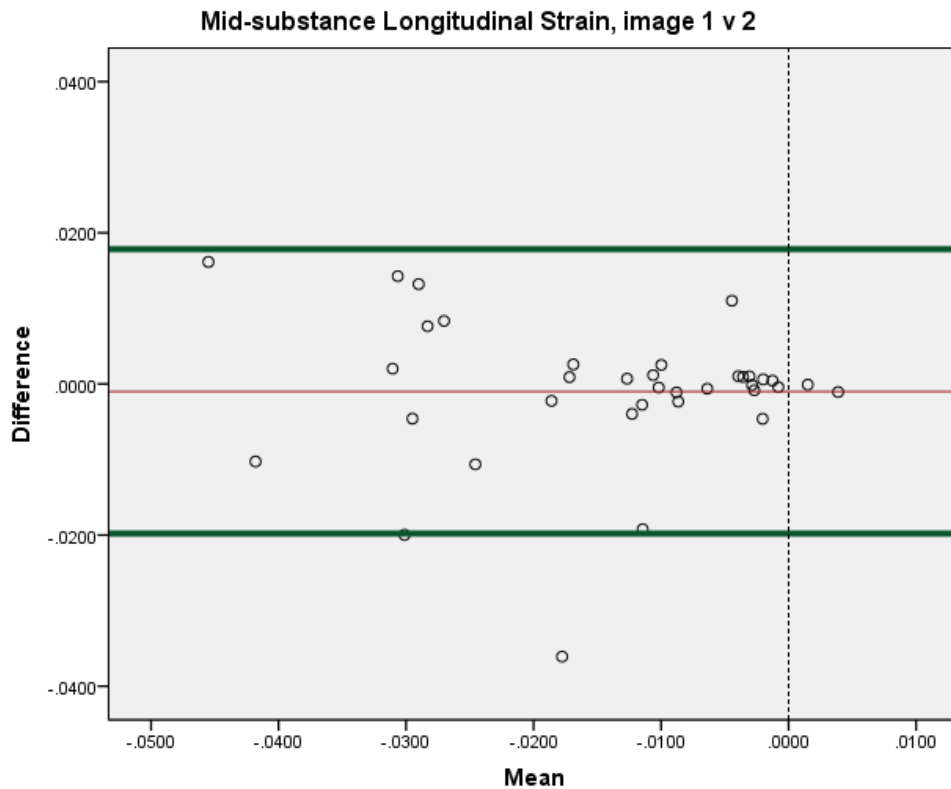


Figure 25. Bland-Altman of Mid-substance Longitudinal strains for Image 1 and Image 2
 Bland-Altman plot of the Mid-substance Longitudinal Strains between image 1 and image 2. The x axis, Mean, is the mean of the values of images 1 and 2. The y axis, Difference, is the difference between image 1 and image 2. The red horizontal line represents the mean of the differences, or the mean of the y axis values. The two green horizontal lines represent the mean of the differences plus or minus two standard deviations, or the 95% confidence interval of the mean difference. The dotted vertical line represents zero mean strain.

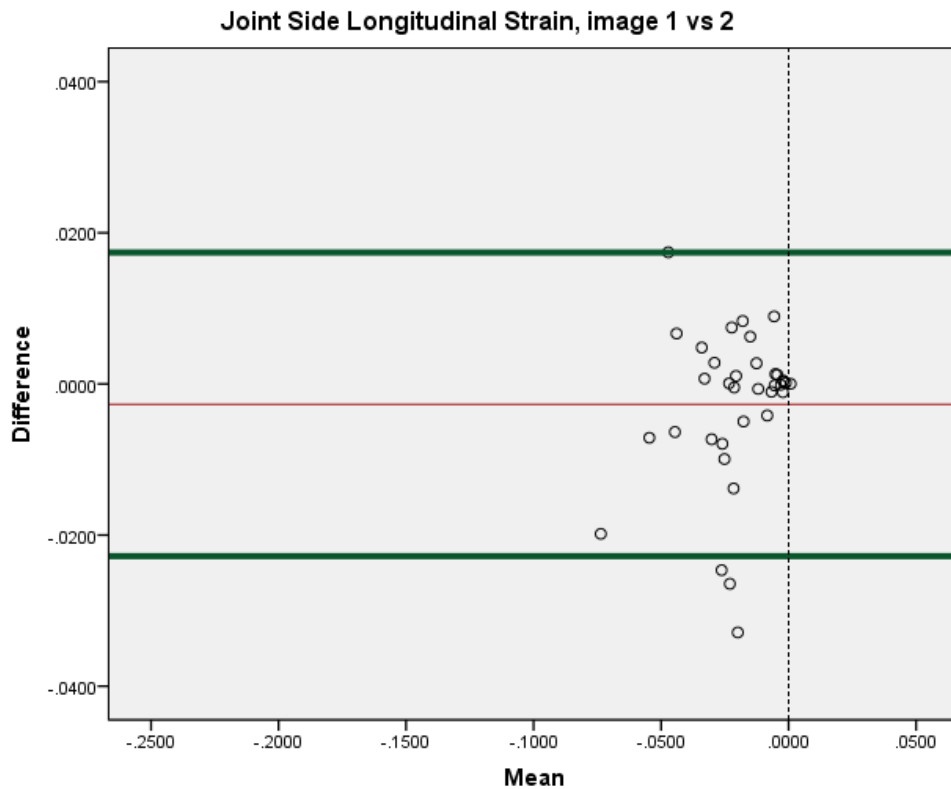


Figure 26. Bland-Altman of Joint side Longitudinal strains for Image 1 and Image 2
 Bland-Altman plot of the Joint Side Longitudinal Strains between image 1 and image 2. The x axis, Mean, is the mean of the values of images 1 and 2. The y axis, Difference, is the difference between image 1 and image 2. The red horizontal line represents the mean of the differences, or the mean of the y axis values. The two green horizontal lines represent the mean of the differences plus or minus two standard deviations, or the 95% confidence interval of the mean difference. The dotted vertical line represents zero mean strain.

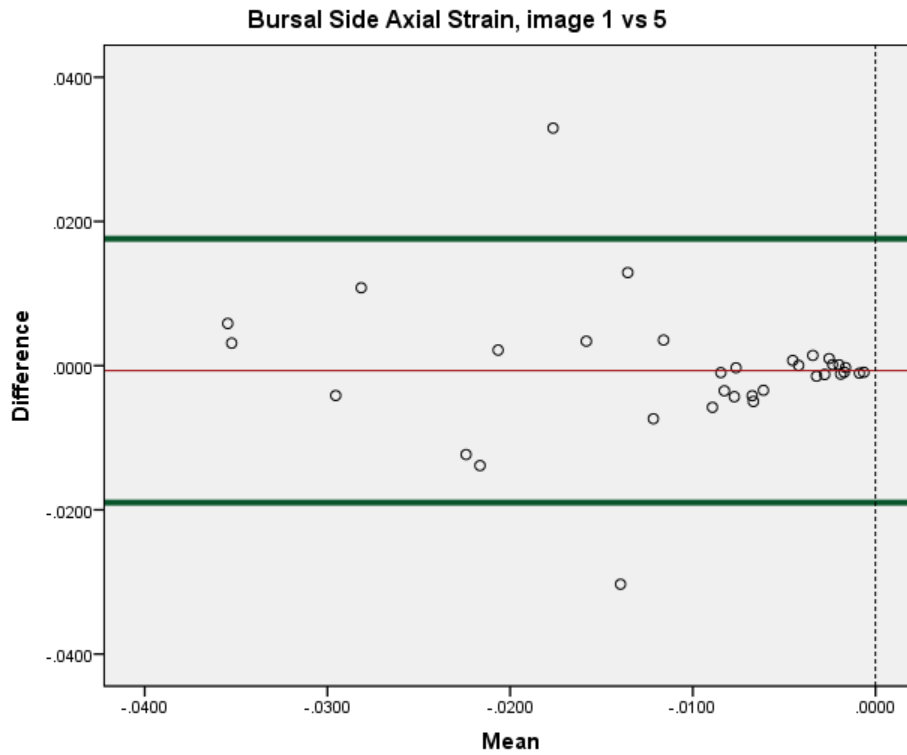


Figure 27. Bland-Altman of Bursal side Axial strains for Image 1 and Image 5
 Bland-Altman plot of the Bursal Side Axial Strains between image 1 and image 5. The x axis, Mean, is the mean of the values of images 1 and 5. The y axis, Difference, is the difference between image 1 and image 5. The red horizontal line represents the mean of the differences, or the mean of the y axis values. The two green horizontal lines represent the mean of the differences plus or minus two standard deviations, or the 95% confidence interval of the mean difference. The dotted vertical line represents zero mean strain.

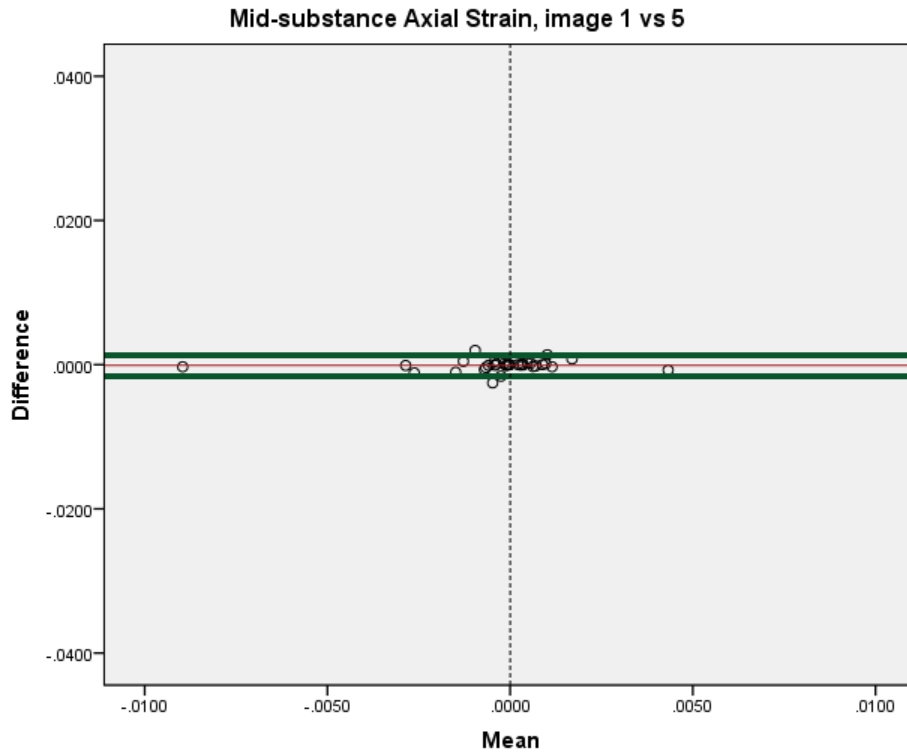


Figure 28. Bland-Altman of Mid-substance Axial strains for Image 1 and Image 5
Bland-Altman plot of the Mid-substance Axial Strains between image 1 and image 5. The x axis, Mean, is the mean of the values of images 1 and 5. The y axis, Difference, is the difference between image 1 and image 5. The red horizontal line represents the mean of the differences, or the mean of the y axis values. The two green horizontal lines represent the mean of the differences plus or minus two standard deviations, or the 95% confidence interval of the mean difference. The dotted vertical line represents zero mean strain.

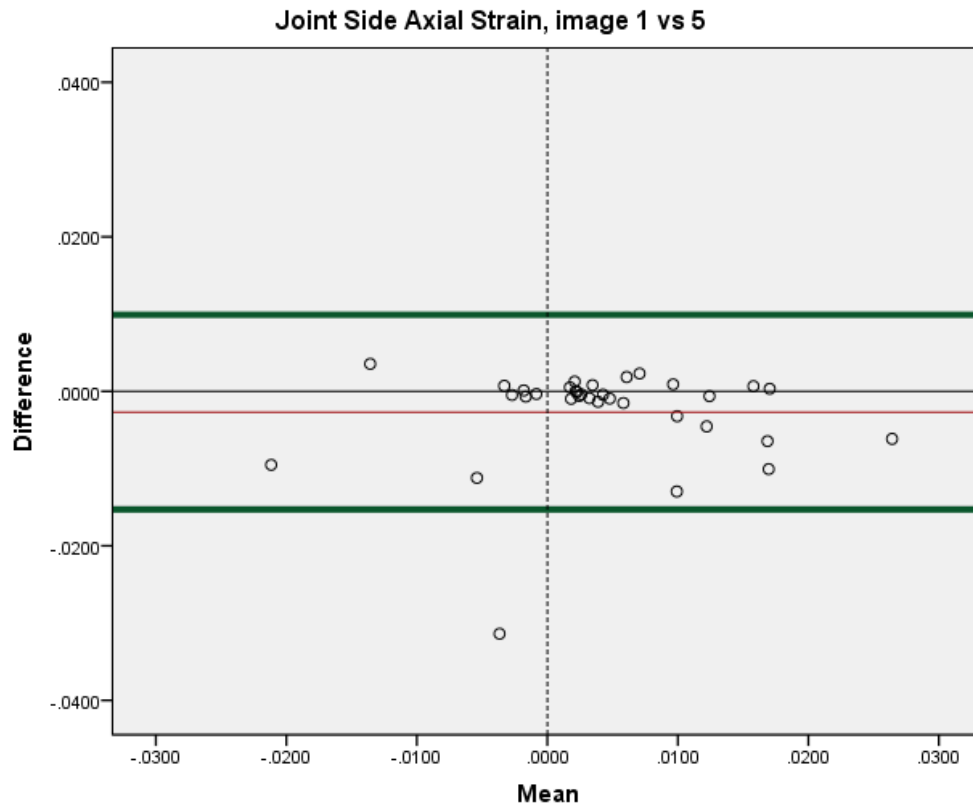


Figure 29. Bland-Altman of Joint side Axial strains for Image 1 and Image 5

Bland-Altman plot of the Joint Side Axial Strains between image 1 and image 5. The x axis, Mean, is the mean of the values of images 1 and 5. The y axis, Difference, is the difference between image 1 and image 5. The red horizontal line represents the mean of the differences, or the mean of the y axis values. The two green horizontal lines represent the mean of the differences plus or minus two standard deviations, or the 95% confidence interval of the mean difference. The dotted vertical line represents zero mean strain.

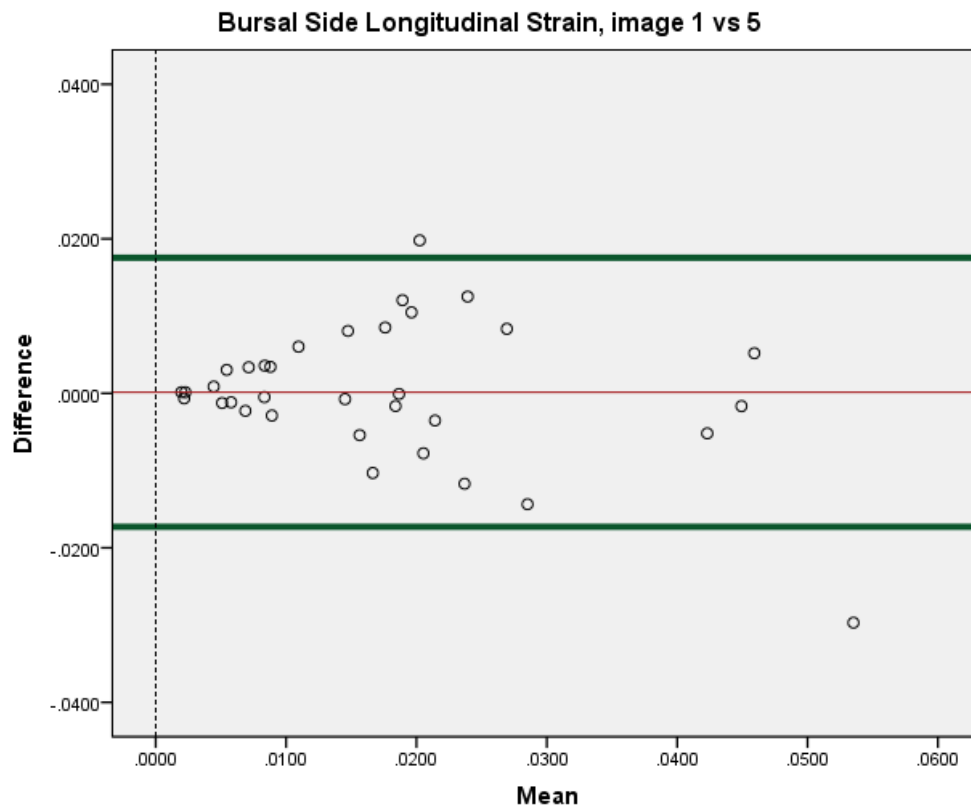


Figure 30. Bland-Altman of Bursal side Longitudinal strains for Image 1 and Image 5
 Bland-Altman plot of the Bursal Side Longitudinal Strains between image 1 and image 5. The x axis, Mean, is the mean of the values of images 1 and 5. The y axis, Difference, is the difference between image 1 and image 5. The red horizontal line represents the mean of the differences, or the mean of the y axis values. The two green horizontal lines represent the mean of the differences plus or minus two standard deviations, or the 95% confidence interval of the mean difference. The dotted vertical line represents zero mean strain.

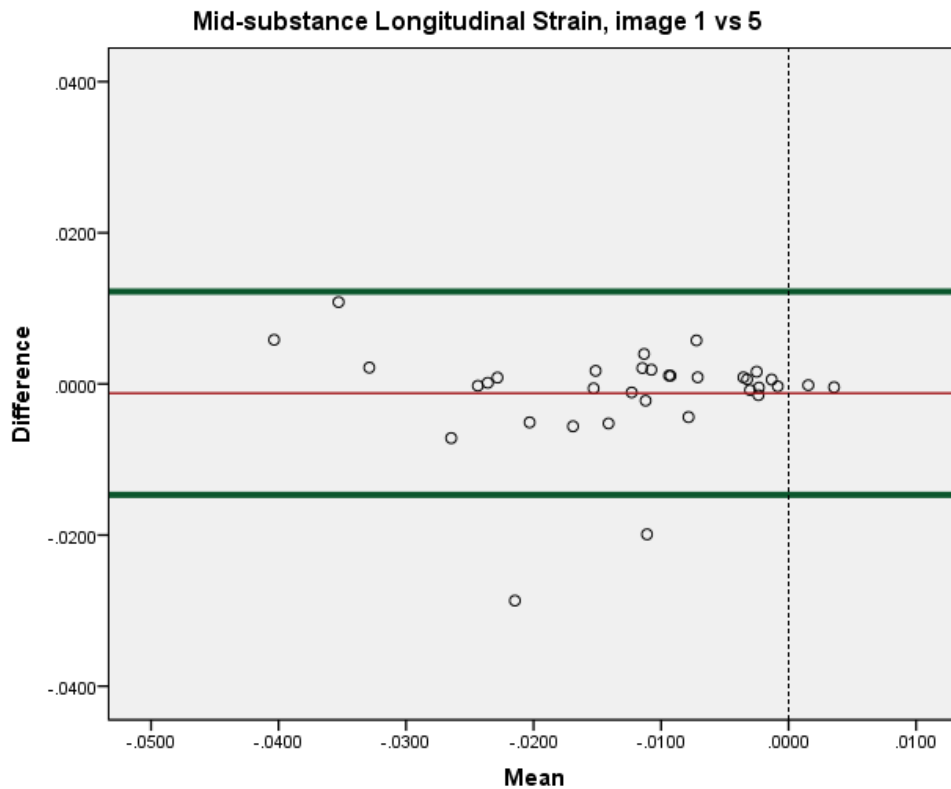


Figure 31. Bland-Altman of Mid-substance Longitudinal strains for Image 1 and Image 5
 Bland-Altman plot of the Mid-substance Longitudinal Strains between image 1 and image 5. The x axis, Mean, is the mean of the values of images 1 and 5. The y axis, Difference, is the difference between image 1 and image 5. The red horizontal line represents the mean of the differences, or the mean of the y axis values. The two green horizontal lines represent the mean of the differences plus or minus two standard deviations, or the 95% confidence interval of the mean difference. The dotted vertical line represents zero mean strain.

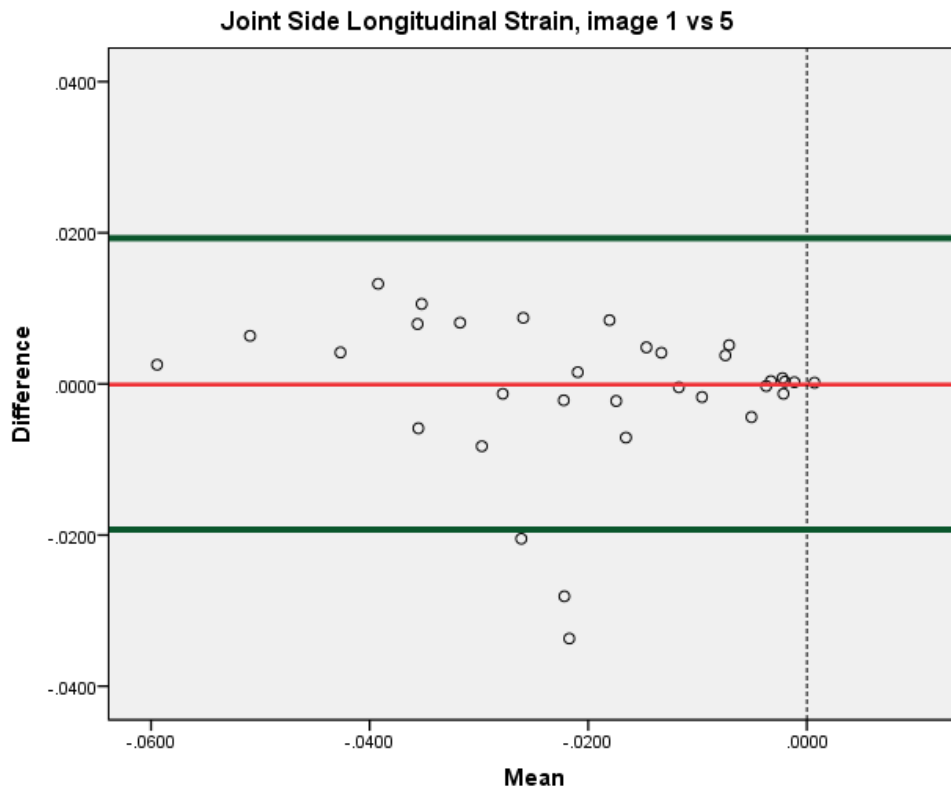


Figure 32. Bland-Altman of Joint side Longitudinal strains for Image 1 and Image 5
 Bland-Altman plot of the Joint Side Longitudinal Strains between image 1 and image 5. The x axis, Mean, is the mean of the values of images 1 and 5. The y axis, Difference, is the difference between image 1 and image 5. The red horizontal line represents the mean of the differences, or the mean of the y axis values. The two green horizontal lines represent the mean of the differences plus or minus two standard deviations, or the 95% confidence interval of the mean difference. The dotted vertical line represents zero mean strain.

CHAPTER 5

DISCUSSION

The purpose of the current study was to examine the reliability of strain measurement of the supraspinatus tendon during an isometric contraction using ultrasound speckle tracking. The investigation tested the hypothesis that ultrasound speckle tracking would provide consistent measures of strain in the supraspinatus tendon during maximal isometric contraction. The very good ICC values, no evidence of systematic error, and low measurement error found in this investigation provides evidence to support the hypothesis that speckle tracking of ultrasound images produces reliable and precise measurements of strain of the supraspinatus tendon during an isometric contraction.

Large loss in data or exclusions of participants can negatively affect the outcomes of a study. The data from 9 participants (21.4%) of the 42 participants involved in the current study were not used in this study. The data from one participant were not used because only four images were able to be collected from the participant. Eight participants were excluded because, during the seed phase of the speckle tracking process, no placement could be made. The reason for the eight participants being excluded for no seed placement being able to be made during the analysis process could be due to: the ultrasound image collector moved the probe during the image collection, the participant's shoulder was not properly stabilized, or the speckle tracking analysis was not performed appropriately. Seven (7) of the nine excluded participants were among the first 12 participants in the study; the remaining two participants were among the first 19 participants in the study. The 9 excluded participants were among the first half of participants in the study, so there was likely a learning effect of the investigators with the procedures. The data from 31 participants were used for statistical analysis, which meets the minimum

requirement of 30 participants to appropriately assume that the data will be a normal distribution for the statistical analysis. The excluded data of this current study could have an effect on the analysis of this current study, since a large percentage (21.4%) of all subjects were either excluded or their data were not used. There is a need for improvement in the methods in this current study and experience of the investigator collecting the ultrasound images.

The ICC values for the longitudinal and axial strains of both within and between images were high (>0.9) for all locations within the tendon (Bursal side, mid-substance, and Joint side). The ICC values greater than 0.9 demonstrate very good reliability (Poiraudau et al., 2001). The high between trial and within trial ICC values suggests that speckle tracking of ultrasound images produce reliable measures of strain within the supraspinatus tendon during an isometric contraction. The magnitude of the mean strain ranged 0.35 to 2.12% for the intra-image measurements and was a range 0.030 to 1.941% for inter-image measurements. The 95% confidence interval for the SEM ranged 0.052 to 0.327% for intra-image measurements and 0.045 to 0.631% for inter-image measurements. The 95% confidence interval for the MDC ranged 0.074 to 0.463% for intra-image measurements and 0.405 to 0.892% for inter-image measurements. The 95% confidence interval for the SEM, as a percentage of the mean strain, ranged 15.0 to 148.6% for intra-image and 32.5 to 150.0% for inter-image. The 95% confidence interval for the MDC, as a percentage of the mean strain, ranged 21.3 to 211.4% for intra-image and 46.0 to 213.3% for inter-image. The 95% confidence interval for the MDC, and therefore the SEM, was relatively large compared to the mean values of strain. The MDC being large relative to the mean strain values suggests there is a lack of precise measurements for all measurements. The reliability of the strain measurements in the current study are very good; however, the precision of the strain measurements needs to improve. The measurement error

found in the current study is relatively high for all measurements, which can be improved by the ultrasound image collector gaining more experience and refining the procedures.

The locations of greatest strain within the tendon may be an indication of the regions most likely to be injured or develop disease. For the longitudinal direction, the greatest stretching was on the bursal side (positive strain) and greatest compression was at the joint side (negative strain). The axial strain was greatest in compression at the bursal side (negative strain) and the greatest stretching at the joint side (positive strain). Longitudinal stretching occurred on the bursal side and longitudinal compression occurred on the joint side of the tendon, as indicated by the longitudinal strain on the bursal side being positive and the joint side being negative. Axial compression occurred on the bursal side and axial stretching occurred on the joint side, as indicated by the axial strain on the bursal side being negative and the joint side being positive. In both directions, the mid-substance was compressing, but the strain was smaller at the mid-substance than at the bursal or joint sides of the tendon. The region of the supraspinatus tendon most likely to develop a tear is the joint side of the anterior border (Ueda et al., 2019). The region of the supraspinatus tendon most likely to develop a tear, the joint side of the anterior border, is the same region that was found to have the largest axial and longitudinal strain in this current study.

Though few studies have measured the strain of the supraspinatus tendon, current studies do not match the strain magnitudes of this study. Kim et al. (2011), utilized ultrasound speckle tracking to investigate supraspinatus tendon strain in vivo during an isometric contraction; tendon strain ranged from 3.4 to 17.0%, with greater strains being reported on the bursal side of the tendon (Kim et al., 2011). The current study also found greater bursal side strains; however, the strains reported by Kim et al. were of greater magnitude. Slagmolen et al. (2012) identified

several challenges, such as how the shoulder and ultrasound image was stabilized to ensure a high quality and appropriate image, to internal and external validity of the Kim et al. paper. Many of the challenges identified by Slagmolen et al. (2012) were addressed in the current study and are likely the explanation to the lower strain measured reported by the current study. In a cadaveric study, Bey, Song, Wehrli, and Soslowky (2002) found the strain of the supraspinatus tendon ranged from 0.9 to 2.5%, which are higher than the strains found in the current study except for the smallest strain, 0.9%, reported by Bey et al. Bey et al. (2002) applied a 34N load to the supraspinatus tendon, which could be greater than the load the participants of the current study applied, resulting in greater strains reported by Bey et al. Bey et al. (2002) also found greater strain measures on the bursal side of the supraspinatus tendon. Though the magnitudes of strain of previous studies do not match the magnitudes of strain of the current study, the location of largest strain of the supraspinatus tendon, which was the bursal side, was consistent.

During the ultrasound imaging procedure, the ultrasound probe was located over the anterior aspect of the supraspinatus tendon. The area of greatest strain measurements identified in the current study corresponds with the location of the highest prevalence of rotator cuff tears, reported by Ueda et al. (2019), the bursal side of the anterior aspect of the supraspinatus tendon. The bursal side of the anterior aspect of the supraspinatus tendon may experience the greatest strain and be the location of the highest prevalence of rotator cuff tears, because of tensile loading and compression of the tendon under the acromion during humeral abduction.

The strain within a tendon, resulting from muscle contraction, may vary amongst tendons, and the reason may be because of differences in tendon tissue composition or differences in maximum force of the movement or task. Arya and Kulig (2010) determined average strain values within the Achilles tendon were approximately 4.36%, which are greater

than all strain values found in this current study. Pearson et al. (2014) determined mean strain values of the patellar tendon ranged from 3.7 to 7.9%, which are larger than all strain values found in this current study. The magnitudes of the strain values reported for the Achilles and patellar tendons, in almost all cases, are larger than the magnitudes of the supraspinatus strain values reported in the current study. The strain of the Achilles and patellar tendons may be larger than the strain of the supraspinatus because of the tensile load of the muscle contraction force on the Achilles tendon compared to the tensile and compressive forces on the supraspinatus tendon during the isometric contraction of the supraspinatus muscle. The loading differences may be a results of muscle size, tendon composition, or tendon dimensions. From comparing measurements and result of this study to previous studies, measured strain does not result in similar magnitudes as the reported strain values of Achilles or patellar tendon studies; which may be the result of the different tissue composition of the tendons, such as collagen, elastin, or proteoglycans.

The Achilles and patellar tendons may be more compliant, and therefore have a greater strain value than the supraspinatus tendon, due to differences in protein composition amongst the tendons. Most tendons are composed of approximately 70-80% collagen, of the dry weight of the tendon, 1 to 2%, elastin of the dry weight of the tendon, proteoglycans, glycosaminoglycan, and other molecules (Hess, Cappiello, Poole, & Hunter, 1989; Kannus, 2000; Ribbans & Collins, 2013; G. P. Riley et al., 1994; Wang et al., 2013). The supraspinatus tendon, which is made up of approximately 95% type I collagen, has a higher type I collagen content percentage than the Achilles or patellar tendons, which each is made up of approximately 80 – 85% type I collagen (Bank et al., 1999; Eleswarapu, Responde, & Athanasiou, 2011; Maffulli, Binfield, & King, 1998; Ribbans & Collins, 2013; G. P. Riley et al., 1994). Differences in the collagen makeup of

tendon could lead to differences in the elastic module, or how much a material resists stretching, of the tendon, which would lead to differences in the magnitude of strain (Shen, Kahn, Ballarini, & Eppell, 2011). Tendon loaded with larger forces, such as the Achilles or patellar tendons, may synthesize more elastin and proteoglycans than tendon loaded with smaller forces, such as the supraspinatus tendon (Batson et al., 2003; Birch, 2007). Tendon proteoglycans regulate fibrillogenesis of collagen and oppose compressive and tensile loading forces (Yoon & Halper, 2005). Proteoglycans indirectly lead to differences in magnitude of strain by regulating the fibrillogenesis of collagen, and proteoglycans directly lead to differences in the magnitude of strain by opposing compressive and tensile loads. Elastin serves to allow tissue to stretch and deform by recoiling back into the original, or near original, state of the tissue before the deformation (Muiznieks, Weiss, & Keeley, 2010). An increased amount of elastin in tendon would make the tendon more elastic, allowing the tendon to store more energy or have a higher elastic module. Differences in the makeup of different tendons, such as the types and amounts of collagen, proteoglycans, and elastin, may lead to differences in strain values of tendon; however, differences in strain values of tendon may also be due to load requirements for movements, such that jumping will have a higher load on the Achilles tendon than raising an arm would on the supraspinatus tendon.

Participants of the current study performed 5 maximal isometric supraspinatus contractions. The contractions were performed with a minimum of 30-second rest between trials. However, minimal effect of repeated muscle contraction on tendon strain was found. Student t-tests were performed to test the differences in supraspinatus tendon strain between trials. Out of the 12 t-tests, only one, the difference joint side axial strain between trials 1 and 5, was statistically different than zero. The increased compliance or stretching of the tendon

between trial 1 and 5 may indicate a hysteresis, such that the mechanical characteristics of the tendon change during repeated movements. The lack of statistically significant differences between trials 1 and 5 suggest that the tendon did not experience a hysteresis.

Review of the Bland-Altman plots revealed systematic error. Twenty-two (22) data points, of the 432 data points, were outside of the 2-standard deviation lines of the Bland-Altman plots. For the longitudinal strain on the bursal side, there is a pattern of greater differences in strain between image 1 and image 5 with increasing strain, suggesting that there is systematic error. There were no other patterns of systematic error identified in the remaining Bland Altman plots. The source of the limited systematic error identified in the current study could be explained by tendon hysteresis; however, there is limited evidence that the hysteresis occurred. The finding of the systematic error found in the longitudinal strain on the bursal side is likely a spurious finding.

Movement of the shoulder presented problems for ultrasound imaging and speckle tracking during the pilot study. This study investigated strain during an isometric contraction of the supraspinatus; to ensure the contraction was isometric, the participant's scapula and arm needed to be stabilized during the contraction in order to prevent movement. Movement of the shoulder could also prevent appropriate ultrasound images from being taken and prevent the speckle tracking process from being completed. For images of participants that did not have their shoulder stabilized, the seed placement, during the setting of the seed during the speckle tracking process, in the current image was either out of bounds of the region of interest or no placement could be made. In combination with holding the participant's arm down to prevent abduction of the shoulder, stabilizing a participant's shoulder reduced gross movement of the

scapula and humerus. The reduction in movement of the scapula and humerus improved the ultrasound imaging and speckle tracking analysis by reducing error.

Limitations

Limitations in the design of the current study persist, even though this study effectively determined the reliability and precision of strain measurements in the supraspinatus tendon of healthy participants.

The potential misalignment between the orientation of the ultrasound images and the determined directions for strain, longitudinal (x) and axial (y), may lead to strain results that do not match perfectly with the true longitudinal and axial strains. This limitation was addressed by lining up the supraspinatus tendon image so that the fibers of the tendon were aligned with the longitudinal direction.

Nine total participants (21.4%) were excluded from this study. All nine excluded participants were among the first 19 participants in this current study. The remaining 22 participants had no exclusions among them. For one excluded participant, only four ultrasound images were collected; an error was made during the image collection process. For the other eight excluded participants, the speckle tracking process could not be completed due to no seed being able to be placed. This seed placement error may come about from poor images or too much movement, either of which would have made the DIC analysis useless or impossible. The poor images or movement may have been due to a novice at ultrasound imaging learning and getting better at ultrasound imaging, since all nine excluded participants occurred within the first 19 participants and there were no exclusions of the last 22 participants. Too much movement of the shoulder or ultrasound probe would have caused the DIC analysis to show no movement or movement to a region that would make no sense, such as into bone. The DIC analysis might

show no movement since no space within the region of interest would have a high enough image correlation to be tracked. Poor images would have prevented the DIC analysis from being completed since the images would have no consistency in the grey scale pattern. These exclusions limited the study in that nine fewer participants' data were used, which could have increased the power of this study. Having 21.4% of all participants excluded from the study limits the reliability and the usefulness of the speckle tracking procedure of this study. To improve the procedures of this current study, the investigator performing the ultrasound imaging should gain more experience and investigators should make sure that the participant's shoulder is stabilized.

The supraspinatus tendon may have become more compliant throughout the five isometric shoulder abductions, which could have led to strain results that might not be consistent for each measurement or would be different from the strain results of unfatigued, unstressed tendon. The mean tendon strain of the fifth image was greater for all of the axial strain measurements and the mid-substance longitudinal strain measurement than the mean tendon strain of the first image. This difference in strain from the first to the fifth image suggests that the tendon was more compliant axially in the last measurement than compared to the first measurement. The change in the compliance of the tendon from the first image to the fifth image shows that there may have been changes in the supraspinatus tendon, such as: change in water content or make up or better motor unit recruitment. Changes in the supraspinatus tendon, such as the tendon stretching more after repeated movements, need to be controlled for, because those changes may affect the results or the interpretation of the results. Changes in the supraspinatus tendon could be controlled by having the participant do warm-up stretches so that their tendon is more compliant.

Future Research

Future research should investigate the validity of using ultrasound speckle tracking of the supraspinatus tendon to measure strain by comparing speckle tracking strain values with physically measured values of strain. The validity of supraspinatus tendon strain measurements has not been explored with ultrasound speckle tracking. Showing evidence for the validity of using ultrasound speckle tracking of the supraspinatus tendon to measure strain would help to make reported strain values more trustworthy.

Participants who are obese, have shoulder pain, or have symptomatic shoulder disease or injury may increase the difficulty of capturing consistent ultrasound images of the thickest portion of the supraspinatus tendon. A study investigating the reliability and precision of using ultrasound speckle tracking of the supraspinatus tendon to measure strain in participants who are morbidly obese, have shoulder pain, or have symptomatic shoulder disease or injury would improve the usefulness or applicability of the method.

Conclusion

The ICC values for all measurements of strain in this study were very good (>0.9). The very good ICC values suggest that the strain measurements made in the current study are reliable for repeated measurement of supraspinatus tendon strain from a single image and for measuring strain of multiple images of a single participant. The SEM values for all measurements of strain were relatively high compared to the strain values. The relatively high SEM values suggest that the measurements of strain of this study are not precise for multiple measurements of the same image or for measurements of different images. Though the methods designed in this study do not provide a perfect candidate for making in vivo measurements of strain of the supraspinatus tendon, the methods in this study can be improved. Significant improvements need to be made

in the procedures and the experience of the investigator collecting the images. The improvements that need to be made in the procedures include refining the technique of stabilizing a participant's scapula and improving ultrasound image quality through more experience in the ultrasound image collector. If these improvements are made, speckle tracking analysis may become a new tool to assess and study healthy and diseased rotator cuff.

REFERENCES

- Ab Ghani, A., Ali, M. B., DharMalingam, S., & Mahmud, J. (2016). Digital image correlation (DIC) technique in measuring strain using opensource platform Ncorr. *Journal of Advanced Research in Applied Mechanics*, 26(6), 10-21.
- Alexander, R. M. (2002). Tendon elasticity and muscle function. *Comp Biochem Physiol A Mol Integr Physiol*, 133(4), 1001-1011.
- Amundsen, B. H., Helle-Valle, T., Edvardsen, T., Torp, H., Crosby, J., Lyseggen, E., . . . Slordahl, S. A. (2006). Noninvasive myocardial strain measurement by speckle tracking echocardiography: validation against sonomicrometry and tagged magnetic resonance imaging. *J Am Coll Cardiol*, 47(4), 789-793. doi:10.1016/j.jacc.2005.10.040
- Andarawis-Puri, N., Ricchetti, E. T., & Soslowky, L. J. (2009). Rotator cuff tendon strain correlates with tear propagation. *J Biomech*, 42(2), 158-163. doi:10.1016/j.jbiomech.2008.10.020
- Arya, S., & Kulig, K. (2010). Tendinopathy alters mechanical and material properties of the Achilles tendon. *J Appl Physiol (1985)*, 108(3), 670-675. doi:10.1152/jappphysiol.00259.2009
- Bank, R. A., TeKoppele, J. M., Oostingh, G., Hazleman, B. L., & Riley, G. P. (1999). Lysylhydroxylation and non-reducible crosslinking of human supraspinatus tendon collagen: changes with age and in chronic rotator cuff tendinitis. *Ann Rheum Dis*, 58(1), 35-41. doi:10.1136/ard.58.1.35
- Batson, E. L., Paramour, R. J., Smith, T. J., Birch, H. L., Patterson-Kane, J. C., & Goodship, A. E. (2003). Are the material properties and matrix composition of equine flexor and extensor tendons determined by their functions? *Equine Veterinary Journal*, 35(3), 314-318.
- Bey, M. J., Song, H. K., Wehrli, F. W., & Soslowky, L. J. (2002). Intratendinous strain fields of the intact supraspinatus tendon: the effect of glenohumeral joint position and tendon region. *J Orthop Res*, 20(4), 869-874. doi:10.1016/S0736-0266(01)00177-2
- Birch, H. L. (2007). Tendon matrix composition and turnover in relation to functional requirements. *Int J Exp Pathol*, 88(4), 241-248. doi:10.1111/j.1365-2613.2007.00552.x
- Blaber, J., Adair, B., & Antoniou, A. (2015). Ncorr: open-source 2D digital image correlation matlab software. *Experimental Mechanics*, 55(6), 1105-1122.
- Cholewinski, J. J., Kusz, D. J., Wojciechowski, P., Cielinski, L. S., & Zoladz, M. P. (2008). Ultrasound measurement of rotator cuff thickness and acromio-humeral distance in the diagnosis of subacromial impingement syndrome of the shoulder. *Knee Surgery, Sports Traumatology, Arthroscopy*. doi:10.1007/s00167-007-0443-4

- Clark, J. M., & Harryman, D. T. (1992). Tendons, ligaments, and capsule of the rotator cuff. Gross and microscopic anatomy. *Journal of Bone and Joint Surgery - Series A*. doi:10.2106/00004623-199274050-00010
- Crass, J. R., Craig, E. V., Bretzke, C., & Feinberg, S. B. (1985). Ultrasonography of the rotator cuff. *Radiographics: a review publication of the Radiological Society of North America, Inc.* doi:10.1148/radiographics.5.6.3916822
- D'hooge, J. (2008). Principles and Different Techniques for Speckle Tracking. *Myocardial Imaging: Tissue Doppler and Speckle Tracking*. doi:10.1002/9780470692448.ch2
- Dugas, J. R., Campbell, D. A., Warren, R. F., Robie, B. H., & Millett, P. J. (2002). Anatomy and dimensions of rotator cuff insertions. *Journal of Shoulder and Elbow Surgery*. doi:10.1067/mse.2002.126208
- Ecklund, K. J., Lee, T. Q., Tibone, J., & Gupta, R. (2007). Rotator cuff tear arthropathy. *Journal of the American Academy of Orthopaedic Surgeons*. doi:10.5435/00124635-200706000-00003
- Eleswarapu, S. V., Responde, D. J., & Athanasiou, K. A. (2011). Tensile properties, collagen content, and crosslinks in connective tissues of the immature knee joint. *PLoS One*, 6(10), e26178. doi:10.1371/journal.pone.0026178
- Grassi, W., Filippucci, E., & Busilacchi, P. (2004). Musculoskeletal ultrasound. *Best Practice and Research: Clinical Rheumatology*. doi:10.1016/j.berh.2004.05.001
- Heimdal, A. (2008). Technical Principles of Tissue Velocity and Strain Imaging Methods. *Myocardial Imaging: Tissue Doppler and Speckle Tracking*, 150-161. doi:10.1002/9780470692448.ch12
- Hess, G. P., Cappiello, W. L., Poole, R. M., & Hunter, S. C. (1989). Prevention and treatment of overuse tendon injuries. *Sports Med*, 8(6), 371-384. doi:10.2165/00007256-198908060-00005
- Jacobson, J. A. (2011). Shoulder US: anatomy, technique, and scanning pitfalls. *Radiology*, 260(1), 6-16. doi:10.1148/radiol.11101082
- Jozsa, L., & Kannus, P. (1997). Tendon Anatomy and Physiology. *Human tendons: anatomy physiology and pathology*. doi:10.1111/j.1600-0838.1997.tb00119.x
- Kannus, P. (2000). Structure of the tendon connective tissue. *Scand J Med Sci Sports*, 10(6), 312-320.
- Karthikeyan, S., Rai, S. B., Parsons, H., Drew, S., Smith, C. D., & Griffin, D. R. (2014). Ultrasound dimensions of the rotator cuff in young healthy adults. *Journal of Shoulder and Elbow Surgery*. doi:10.1016/j.jse.2013.11.012

- Kendall, F. P., McCreary, E. K., & Provance, P. G. (1993). *Muscles Testing and Function* (4th ed.). Philadelphia.: Lippincott, Williams and Wilkins.
- Kim, Y. S., Kim, J. M., Bigliani, L. U., Kim, H. J., & Jung, H. W. (2011). In vivo strain analysis of the intact supraspinatus tendon by ultrasound speckles tracking imaging. *Journal of Orthopaedic Research*. doi:10.1002/jor.21470
- Kjær, M., Langberg, H., Heinemeier, K., Bayer, M. L., Hansen, M., Holm, L., . . . Magnusson, S. P. (2009). From mechanical loading to collagen synthesis, structural changes and function in human tendon. *Scandinavian Journal of Medicine and Science in Sports*. doi:10.1111/j.1600-0838.2009.00986.x
- Korstanje, J. W. H., Selles, R. W., Stam, H. J., Hovius, S. E. R., & Bosch, J. G. (2010). Development and validation of ultrasound speckle tracking to quantify tendon displacement. *Journal of Biomechanics*. doi:10.1016/j.jbiomech.2010.01.001
- Leggin, B. G., Michener, L. A., Shaffer, M. A., Breneman, S. K., Iannotti, J. P., & Williams, G. R. (2006). The Penn shoulder score: reliability and validity. *The Journal of orthopaedic and sports physical therapy*.
- Locke, R. C., Peloquin, J. M., Lemmon, E. A., Szostek, A., Elliott, D. M., & Killian, M. (2017). Strain distribution of intact rat rotator cuff tendon-to-bone attachments and attachments with defects. *Journal of Biomechanical Engineering*. doi:10.1115/1.4038111
- Luime, J. J., Koes, B. W., Hendriksen, I. J. M., Burdorf, A., Verhagen, A. P., Miedema, H. S., & Verhaar, J. A. N. (2004). Prevalence and incidence of shoulder pain in the general population; a systematic review. *Scandinavian Journal of Rheumatology*. doi:10.1080/03009740310004667
- Maeda, E., Shelton, J. C., Bader, D. L., & Lee, D. A. (2007). Time dependence of cyclic tensile strain on collagen production in tendon fascicles. *Biochemical and Biophysical Research Communications*. doi:10.1016/j.bbrc.2007.08.029
- Maffulli, N., Binfield, P. M., & King, J. B. (1998). Tendon problems in athletic individuals. *J Bone Joint Surg Am*, 80(1), 142-144.
- Magnusson, S. P., Langberg, H., & Kjaer, M. (2010). The pathogenesis of tendinopathy: Balancing the response to loading. *Nature Reviews Rheumatology*. doi:10.1038/nrrheum.2010.43
- Martinoli, C. (2010). Musculoskeletal ultrasound: technical guidelines. *Insights Imaging*, 1(3), 99-141. doi:10.1007/s13244-010-0032-9
- Marwick, T. H., Leano, R. L., Brown, J., Sun, J. P., Hoffmann, R., Lysyansky, P., . . . Thomas, J. D. (2009). Myocardial Strain Measurement With 2-Dimensional Speckle-Tracking Echocardiography. Definition of Normal Range. *JACC: Cardiovascular Imaging*. doi:10.1016/j.jcmg.2007.12.007

- McClure, P., Tate, A. R., Kareha, S., Irwin, D., & Zlupko, E. (2009). A clinical method for identifying scapular dyskinesis, part 1: Reliability. *Journal of Athletic Training*. doi:10.4085/1062-6050-44.2.160
- McCreesh, K. M., Purtill, H., Donnelly, A. E., & Lewis, J. S. (2017). Increased supraspinatus tendon thickness following fatigue loading in rotator cuff tendinopathy: Potential implications for exercise therapy. *BMJ Open Sport and Exercise Medicine*. doi:10.1136/bmjsem-2017-000279
- Michener, L. A., Subasi Yesilyaprak, S. S., Seitz, A. L., Timmons, M. K., & Walsworth, M. K. (2013). Supraspinatus tendon and subacromial space parameters measured on ultrasonographic imaging in subacromial impingement syndrome. *Knee Surgery, Sports Traumatology, Arthroscopy*. doi:10.1007/s00167-013-2542-8
- Michener, L. A., Walsworth, M. K., Doukas, W. C., & Murphy, K. P. (2009). Reliability and Diagnostic Accuracy of 5 Physical Examination Tests and Combination of Tests for Subacromial Impingement. *Archives of Physical Medicine and Rehabilitation*. doi:10.1016/j.apmr.2009.05.015
- Miller, R. M., Fujimaki, Y., Araki, D., Musahl, V., & Debski, R. E. (2014). Strain distribution due to propagation of tears in the anterior supraspinatus tendon. *Journal of Orthopaedic Research*. doi:10.1002/jor.22675
- Mondillo, S., Galderisi, M., Mele, D., Cameli, M., Lomoriello, V. S., Zacà, V., . . . Badano, L. (2011). Speckle-Tracking Echocardiography. *Journal of Ultrasound in Medicine*. doi:10.7863/jum.2011.30.1.71
- Muiznieks, L. D., Weiss, A. S., & Keeley, F. W. (2010). Structural disorder and dynamics of elastin. *Biochem Cell Biol*, 88(2), 239-250. doi:10.1139/o09-161
- Neer. (1983). Impingement lesions BT - Clin Orthop. *ClinOrthop*, 173.
- Neer, C. S. (1985). Involuntary inferior and multidirectional instability of the shoulder: etiology, recognition, and treatment. *Instructional course lectures*.
- Park, H. B., Yokota, A., Gill, H. S., El Rassi, G., & McFarland, E. G. (2005). Diagnostic accuracy of clinical tests for the different degrees of subacromial impingement syndrome. *Journal of Bone and Joint Surgery - Series A*. doi:10.2106/JBJS.D.02335
- Pearson, S. J., Ritchings, T., & Mohamed, A. S. A. (2014). Regional strain variations in the human patellar tendon. *Medicine and Science in Sports and Exercise*. doi:10.1249/MSS.0000000000000247
- Poiraudeau, S., Chevalier, X., Conrozier, T., Flippo, R. M., Liote, F., Noel, E., . . . Rhumato, R. (2001). Reliability, validity, and sensitivity to change of the Cochin hand functional disability scale in hand osteoarthritis. *Osteoarthritis Cartilage*, 9(6), 570-577. doi:10.1053/joca.2001.0422

- Reed, D., Cathers, I., Halaki, M., & Ginn, K. (2013). Does supraspinatus initiate shoulder abduction? *Journal of Electromyography and Kinesiology*, 23(2), 425-429.
- Reinold, M. M., Macrina, L. C., Wilk, K. E., Fleisig, G. S., Dun, S., Barrentine, S. W., . . . Andrews, J. R. (2007). Electromyographic analysis of the supraspinatus and deltoid muscles during 3 common rehabilitation exercises. *J Athl Train*, 42(4), 464-469.
- Revell, J., Mirmehdi, M., & McNally, D. (2005). Computer vision elastography: Speckle adaptive motion estimation for elastography using ultrasound sequences. *IEEE Transactions on Medical Imaging*. doi:10.1109/TMI.2005.848331
- Ribbans, W. J., & Collins, M. (2013). Pathology of the Achilles Tendon: do our genes contribute? *The Journal of Bone and Joint Surgery*, 95-B(3), 305-313.
- Richardson, W. J., Kegerreis, B., Thomopoulos, S., & Holmes, J. W. (2018). Potential strain-dependent mechanisms defining matrix alignment in healing tendons. In *Biomechanics and Modeling in Mechanobiology*.
- Riley, G. (2004). The pathogenesis of tendinopathy. A molecular perspective. *Rheumatology*. doi:10.1093/rheumatology/keg448
- Riley, G. P., Harrall, R. L., Constant, C. R., Chard, M. D., Cawston, T. E., & Hazleman, B. L. (1994). Tendon degeneration and chronic shoulder pain: changes in the collagen composition of the human rotator cuff tendons in rotator cuff tendinitis. *Ann Rheum Dis*, 53(6), 359-366. doi:10.1136/ard.53.6.359
- Roh, M. S., Wang, V. M., April, E. W., Pollock, R. G., Bigliani, L. U., & Flatow, E. L. (2000). Anterior and posterior musculotendinous anatomy of the supraspinatus. *Journal of Shoulder and Elbow Surgery*. doi:10.1067/mse.2000.108387
- Screen, H. R. C., Shelton, J. C., Bader, D. L., & Lee, D. A. (2005). Cyclic tensile strain upregulates collagen synthesis in isolated tendon fascicles. *Biochemical and Biophysical Research Communications*. doi:10.1016/j.bbrc.2005.08.102
- Seitz, A. L., McClure, P. W., Finucane, S., Boardman, N. D., & Michener, L. A. (2011). Mechanisms of rotator cuff tendinopathy: Intrinsic, extrinsic, or both? *Clinical Biomechanics*. doi:10.1016/j.clinbiomech.2010.08.001
- Seitz, A. L., & Michener, L. A. (2011). Ultrasonographic measures of subacromial space in patients with rotator cuff disease: A systematic review. *Journal of Clinical Ultrasound*. doi:10.1002/jcu.20783
- Shen, Z. L., Kahn, H., Ballarini, R., & Eppell, S. J. (2011). Viscoelastic properties of isolated collagen fibrils. *Biophys J*, 100(12), 3008-3015. doi:10.1016/j.bpj.2011.04.052
- Shrout, P. E., & Fleiss, J. L. (1979). Intraclass correlations: uses in assessing rater reliability. *Psychol Bull*, 86(2), 420-428.

- Slagmolen, P., Scheys, L., D'Hooge, J., Suetens, P., Peers, K., Debeer, P., & Bellemans, J. (2012). In regard to: "in vivo strain analysis of the intact supraspinatus tendon by ultrasound speckles tracking imaging". *Journal of Orthopaedic Research*, 29(12), 1931-1937. doi:10.1002/jor.22174
- Slane, L. C., Bogaerts, S., Thelen, D. G., & Scheys, L. (2018). Nonuniform deformation of the patellar tendon during passive knee flexion. *Journal of Applied Biomechanics*. doi:10.1123/jab.2017-0067
- Slane, L. C., & Thelen, D. G. (2015). Achilles tendon displacement patterns during passive stretch and eccentric loading are altered in middle-aged adults. *Medical Engineering and Physics*. doi:10.1016/j.medengphy.2015.04.004
- Speer, K. P., Hannafin, J. A., Altchek, D. W., & Warren, R. F. (1994). An Evaluation of the Shoulder Relocation Test. *The American Journal of Sports Medicine*. doi:10.1177/036354659402200205
- Stratford, P. W. (2004). Getting more from the literature: estimating the standard error of measurement from reliability studies. *Physiotherapy Canada*, 56(1), 27-30.
- Tada, H., Paris, P. C., & Irwin, G. R. (2000). Part 1: Introductory Information. In *The Stress Analysis of Crack Handbook* (3rd ed., pp. 2-26). New York: American Society of Mechanical Engineers.
- Tate, A. R., McClure, P., Kareha, S., Irwin, D., & Barbe, M. F. (2009). A clinical method for identifying scapular dyskinesis, part 2: Validity. *Journal of Athletic Training*. doi:10.4085/1062-6050-44.2.165
- Taylor, D. C., Dalton, J. D., Seaber, A. V., & Garrett, W. E. (1990). Viscoelastic properties of muscle-tendon units: The biomechanical effects of stretching. *The American Journal of Sports Medicine*. doi:10.1177/036354659001800314
- Teefey, S. A., Middleton, W. D., & Yamaguchi, K. (1999). Shoulder sonography: State of the art. *Radiologic Clinics of North America*. doi:10.1016/S0033-8389(05)70128-7
- Theobald, P. S., Dowson, D., Khan, I. M., & Jones, M. D. (2012). Tribological characteristics of healthy tendon. *Journal of Biomechanics*, 45, 1972-1978. doi:10.1016/j.jbiomech.2012.05.005
- Ueda, Y., Sugaya, H., Takahashi, N., Matsuki, K., Tokai, M., Hoshika, S., . . . Hamada, H. (2019). Prevalence and Site of Rotator Cuff Lesions in Shoulders With Recurrent Anterior Instability in a Young Population. *Orthop J Sports Med*, 7(6), 2325967119849876. doi:10.1177/2325967119849876
- Van Der Windt, D. A. W. M., Koes, B. W., De Jong, B. A., & Bouter, L. M. (1995). Shoulder disorders in general practice: Incidence, patient characteristics, and management. *Annals of the Rheumatic Diseases*. doi:10.1136/ard.54.12.959

- Van Doesburg, M. H. M., Yoshii, Y., Henderson, J., Villarraga, H. R., Moran, S. L., & Amadio, P. C. (2012). Speckle-tracking sonographic assessment of longitudinal motion of the flexor tendon and subsynovial tissue in carpal tunnel syndrome. *Journal of Ultrasound in Medicine*. doi:10.7863/jum.2012.31.7.1091
- Vecchio, P., Kavanagh, R., Hazleman, B. L., & King, R. H. (1995). Shoulder pain in a community-based rheumatology clinic. *Rheumatology*. doi:10.1093/rheumatology/34.5.440
- Venables, H. (2011). How does ultrasound work? *Ultrasound*. doi:10.1258/ult.2010.010051
- Wakefield, R. J., Balint, P. V., Szkudlarek, M., Filippucci, E., Backhaus, M., D'Agostino, M. A., . . . Conaghan, P. G. (2005). Musculoskeletal ultrasound including definitions for ultrasonographic pathology. *Journal of Rheumatology*. doi:0315162X-32-2485 [pii]
- Wang, T., Gardiner, B. S., Lin, Z., Rubenson, J., Kirk, T. B., Wang, A., . . . Zheng, M. H. (2013). Bioreactor design for tendon/ligament engineering. *Tissue Eng Part B Rev*, 19(2), 133-146. doi:10.1089/ten.TEB.2012.0295
- Warner, J. J. P., Micheli, L. J., Arslanian, L. E., Kennedy, J., & Kennedy, R. (1990). Patterns of flexibility, laxity, and strength in normal shoulders and shoulders with instability and impingement. *The American Journal of Sports Medicine*. doi:10.1177/036354659001800406
- Weir, J. P. (2005). Quantifying test-retest reliability using the intraclass correlation coefficient and the SEM. *Journal of Strength and Conditioning Research*. doi:10.1519/15184.1
- Wickham, J., Pizzari, T., Stansfeld, K., Burnside, A., & Watson, L. (2010). Quantifying 'normal' shoulder muscle activity during abduction. *Journal of Electromyography and Kinesiology*, 20(2), 212-222.
- Willems, P. A., Cavagna, G. A., & Heglund, N. C. (1995). External, internal and total work in human locomotion. *The Journal of Experimental Biology*. doi:10.1007/BF00430237
- Yoon, J. H., & Halper, J. (2005). Tendon proteoglycans: biochemistry and function. *J Musculoskelet Neuronal Interact*, 5(1), 22-34.
- Zajac, F. E. (1989). Muscle and tendon: properties, models, scaling, and application to biomechanics and motor control. *Crit Rev Biomed Eng*, 17(4), 359-411.

APPENDIX A: IRB APPROVAL



Office of Research Integrity
Institutional Review Board
One John Marshall Drive
Huntington, WV 25755

FWA 00002704

IRB1 #00002205

IRB2 #00003206

February 25, 2019

Mark Timmons, PhD
Marshall University, School of Kinesiology

RE: IRBNet ID# 1398864-1
At: Marshall University Institutional Review Board #1 (Medical)

Dear Dr. Timmons:

Protocol Title: [1398864-1] Supraspinatus Stress Strain Relationship during a Maximal Isometric Voluntary Contraction.

Site Location: MU

Submission Type: New Project APPROVED

Review Type: Expedited Review

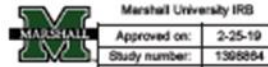
In accordance with 45CFR46.110(a)(4)(6)(7), the above study was granted Expedited approval today by the Marshall University Institutional Review Board #1 (Medical) Chair. An annual update will be required on February 25, 2020 for administrative review and approval. The update must include the Annual Update Form and current educational certificates for all investigators involved in the study. All amendments must be submitted for approval by the IRB Chair prior to implementation and a closure request is required upon completion of the study.

If you have any questions, please contact the Marshall University Institutional Review Board #1 (Medical) Coordinator Trula Stanley at (304) 696-7320 or stanley@marshall.edu. Please include your study title and reference number in all correspondence with this office.

Sincerely,

Bruce F. Day, ThD, CIP
Director, Office of Research Integrity

APPENDIX B: CONSENT FORM



Marshall University
Informed Consent to Participate in a Research Study

**Supraspinatus Stress Strain Relationship during a Maximal Isometric
 Voluntary Contraction.**

Mark K Timmons PhD ATC, Principal Investigator

You are being invited to take part in a research study about tendon stiffness. This study will use ultrasound imaging to measure the stiffness of the rotator cuff tendon. If you participate in this study, you will have several ultrasound images of your shoulder taken and you will perform several maximal contractions of your shoulder muscles.

By doing this study, we hope to develop a better way to measure tendon stiffness. Your participation in this research will last about 1 hour.

The purpose of this research is to use ultrasound to measure tendon stiffness. The information gained will help researchers study the effects of shoulder rehabilitation and the mechanisms that produce shoulder injury. You might feel fatigue and discomfort of your shoulder muscles. For a complete description of risks, refer to the Detailed Consent. You do not have to participate in this study. For a complete description of alternate treatment/procedures, refer to the Detailed Consent.

If you decide to take part in the study, it should be because you really want to volunteer. You will not lose any services, benefits or rights you would normally have if you choose not to volunteer.

For questions about the study or in the event of a research-related injury, contact the study investigator, Mark Timmons at (304) 696-2925. You should also call the investigator if you have a concern or complaint about the research.

For questions about your rights as a research participant, contact the Marshall University Office of Research Integrity at (304) 696-4303.

You will be given a signed and dated copy of this consent form.

SIGNATURES

You agree to take part in this study and confirm that you are 18 years of age or older. You have had a chance to ask questions about being in this study and have had those questions answered. By signing this consent form you are not giving up any legal rights to which you are entitled.

 Subject Name (Printed)

 Subject Signature

 Date

Person Obtaining Consent (Printed)

Person Obtaining Consent Signature

Date

DETAILED CONSENT:

Are There Reasons Why You Would Not Qualify for This Study?

You will be excluded from this study if you currently have shoulder pain, you have had shoulder surgery, you cannot raise your arm over your head, you have arthritis. You will also be excluded from the study if you are younger than 18 or older than 30 years of age

How Many People Will Take Part In The Study?

About 30 people will take part in this study, 40 subjects are the most that would be able to enter the study.

What Is Involved In This Research Study?

During the study, you will first fill out a questionnaire about your shoulder, and then the researcher will perform a brief examination of your shoulder. After the examination, the researcher will use an ultrasound machine to make several images of the shoulder of the arm that you use to write or throw a ball. During the ultrasound imaging, you will need to wear a sleeveless or tank top shirt. During the ultrasound, imaging you will be asked to sit down and your arm will be placed in several positions, you will also be asked to perform several maximal contractions of your shoulder muscles. The questionnaires, shoulder examination, and ultrasound imaging will take about 30 minutes to complete

How Long Will You Be In The Study?

You will be in the study for 1 testing session that will take about 60 minutes to complete.

You can decide to stop participating at any time. If you decide to stop participating in the study we encourage you to talk to the investigators or study staff to discuss what follow up care and testing could be most helpful for you.

The study principal investigator may stop you from taking part in this study at any time if he/she believes it is in your best interest; if you do not follow the study rules; or if the study is stopped.

What Are The Risks Of The Study?

There may be these risks:

Being in this study involves some risk to you. You should discuss the risk of being in this study with the study staff.

You should talk to your study doctor about any side effects that you have while taking part in the study.

Rev 1/30/19

Subject's Initials _____

Risks and side effects related to the testing session include increased shoulder pain, muscle soreness, muscle fatigue and reduced shoulder strength. These risks and side effects are temporary and are no greater than the risks associated with any physical exercise program. These side effects can be reduced by stretching exercises, and applying either moist heat or ice. **If you experience pain that you would describe as being more than 7 out of 10 you should stop the testing session contact your doctor.**

There may also be other side effects that we cannot predict. You should tell the researchers if any of these risks bother or worry you. This may help avoid side effects, interactions and other risks. There are no funds available for compensation for any injury that occurs as a result of your participation in this study.

Are There Benefits To Taking Part In The Study?

If you agree to take part in this study, there may or may not be direct benefit to you. We hope the information learned from this study will benefit other people in the future. The benefits of participating in this study may be: You will gain information about the function of your shoulder.

What About Confidentiality?

We will do our best to make sure that your personal information is kept confidential. However, we cannot guarantee absolute confidentiality. Federal law says we must keep your study records private. Nevertheless, under unforeseen and rare circumstances, we may be required by law to allow certain agencies to view your records. Those agencies would include the Marshall University IRB, Office of Research Integrity (ORI) and the federal Office of Human Research Protection (OHRP). This is to make sure that we are protecting your rights and your safety. If we publish the information, we learn from this study, you will not be identified by name or in any other way.

What Are The Costs Of Taking Part In This Study?

There are no costs to you for taking part in this study. All the study costs, including any study tests, supplies and procedures related directly to the study, will be paid for by the study.

Will You Be Paid For Participating?

You will receive no payment or other compensation for taking part in this study.

What Are Your Rights As A Research Study Participant?

Taking part in this study is voluntary. You may choose not to take part or you may leave the study at any time. Refusing to participate or leaving the study will not result in any penalty or loss of benefits to which you are entitled. If you decide to stop participating in the study, we encourage you to talk to the investigators or study staff first.